Evidence for Aseismic Deformation Rate Changes Prior to Earthquakes*

Evelyn A. Roeloffs

U.S. Geological Survey, Vancouver, Washington 98683; email: evelynr@usgs.gov

Annu. Rev. Earth Planet. Sci.
2006. 34:591–627

First published online as a Review in Advance on January 31, 2006

The *Annual Review of Earth and Planetary Science* is online at earth.annualreviews.org

doi: 10.1146/annurev.earth.34.031405.124947

0084-6597/06/0530-0591$20.00

Key words

geodesy, seismology, subduction, faults, earthquake prediction

Abstract

For ten earthquakes in nonmagmatic settings, there are credible published accounts of pre-earthquake deformation-rate changes lasting hundreds of seconds to more than a decade. Although most $M > 7.5$ earthquakes have occurred without detectable pre-earthquake deformation, the detection threshold for aseismic deformation remains high, in that aseismic slip with moment equivalent to an M5 earthquake would in most (although not all) cases have been missed. Interseismic deformation rates vary without being followed by earthquakes, and a strain-rate change prior to the 1989 M_w6.9 Loma Prieta, California, earthquake is shown to be similar in size to many other rate changes that have occurred since that time. Most examples of pre-earthquake aseismic deformation lasting hundreds of seconds or more probably originate adjacent to, or downdip of, the seismic rupture plane, rather than within the zone that undergoes seismic failure.

INTRODUCTION

Pre-earthquake changes in rates of aseismic crustal deformation could facilitate warnings of impending earthquakes. But actual data documenting deformation rates changing prior to earthquakes are rare. Many earthquake scientists believe such deformation almost never occurs, or will remain undetectable. Here, I describe the best-documented examples of deformation-rate changes prior to earthquakes (**Table 1**), and I summarize available data on selected earthquakes for which no pre-earthquake deformation-rate anomalies were detected (**Table 2**).

Crustal deformation prior to earthquakes can also potentially discriminate between theories of the earthquake generation process. Earthquake scientists agree an earthquake is unlikely until stored strain energy in the crust suffices to supply seismic strain energy release, but a fundamental question remains as to whether some immediate stimulus for seismic slip is also required. Seismic slip may nucleate

Table 1 Earthquakes with pre-earthquake deformation rate changes, in chronological order

	Method of observation	Start time (prior to mainshock)	Equivalent moment magnitude of pre-earthquake slip	References
M9 Cascadia, USA and Canada January 29, 1700	Microfossils	Unknown	Unknown	Shennan et al. 1998
M_s8.2 Tonankai, Japan December 7, 1944	Leveling	1 day	7.8	Sagiya 1998, Linde & Sacks 2002
M_w8.3 Nankaido, Japan December 20, 1946	Tide gauges,water wells	3 days	7.9	Sato 1982, Linde & Sacks 2002
M_w9.2 Chile May 22, 1960	Long-period seismometer	14–20 min	8.9–9.1	Cifuentes & Silver 1989
M_w9.2 Prince William Sound, Alaska March 28, 1964	Microfossils	10–12 years	(0.12 ± 0.13 m uplift)	Hamilton & Shennan 2005
M7.0 Izu-Oshima-Kinkai, Japan January 14, 1978	Leveling, groundwater levels, geodolite, tide gauges	2 years	(15 cm uplift)	Inouchi & Sato 1979, Wakita 1981
M_s6.8 Urakawa-oki, Japan March 21, 1982	Leveling	3–11.5 years	(0.4 m slip)	Taylor et al. 1991; Iio et al. 2002; Murai et al. 2003
M_s7.8 Japan Sea May 26, 1983	Leveling, tide gauges, borehole strain	14 years	7.7	Iio et al. 2002, Mogi 1985
M_w6.1 Kettleman Hills, California August 4, 1985	Water levels, borehole strain	3 days	5.4	Roeloffs & Quilty 1997
M_w7.6 Peru July 7, 2001	CGPS	18 h	7.8	Melbourne & Webb 2002
M3.5 Corinth Rift, Greece December 3, 2002	Borehole strain	1 h	5.3	Bernard et al. 2004

Table 2 Selected instrumented earthquakes for which no pre-earthquake deformation rate changes were detected

	Type of data (distance)	Allowable moment of pre-earthquake slip	References
M_w6.9 Loma Prieta, California October 18, 1989	Borehole strainmeters (40 km), Campaign GPS (0–31 km)	<M5.4	Lisowski et al. 1993
M_w7.3 Landers, California June 28, 1992	Piñon Flat strainmeters, GPS (68 km), Dilatometer (100 km)	<M4.8 (Piñon Flat laser strainmeter)	Wyatt et al. 1994, Johnston et al. 1994
M_w7.6 ChiChi, Taiwan September 21, 1999	CGPS (10 km)	<M6	Yu et al. 2001
M_w7.1 Hector Mine, California October 16, 1999	CGPS (25 km), InSAR	<M6.4 (CGPS), <M5 (InSAR)	Mellors et al. 2002
M_w8.4 Peru June 23, 2001	CGPS (300 km)	<M7.6	Melbourne & Webb 2002
M_w8.3 Tokachi-oki, Japan September 25, 2003	CGPS (30 km from fault plane, 70 km from epicenter)	<M7	Irwan et al. 2004
M_w6.0 Parkfield, California September 28, 2004	Borehole strain (10km)	<M3.2	Langbein et al. 2005

spontaneously on fault patches, where frictional resistance drops with increasing slip or sliding speed (rate- and state-dependent friction, e.g., Dieterich 1992, Ohnaka 1992), without accelerated application of stress. If friction parameters measured in the laboratory are appropriate, this scenario implies pre-earthquake aseismic slip lasting seconds or less, localized near the earthquake hypocenter (Yamashita & Ohnaka 1992). Numerical simulations of faults with rate- and state-dependent friction laws exhibit pre-earthquake accelerating slip detectable by existing instruments if the characteristic slip distance, L, over which frictional resistance falls is much longer than measured in the laboratory. Alternatively, earthquakes may take place while aseismic deformation rates, on subsets of the rupture surface and/or on its along-strike or downdip extensions, have been elevated above background levels by some other means, such as loading by another earthquake.

The seismic nucleation phase—slow moment release lasting up to tens of seconds prior to large earthquakes—represents the beginning of an unstable process within the seismic rupture zone. Beroza & Ellsworth (1996) list 48 earthquakes M1.1 to M8.1, recorded on high-dynamic-range digital seismographs at typical distances of tens of kilometers, that have begun with such phases that contribute about 1% of the total earthquake moment.

In contrast, most observed pre-earthquake deformation-rate changes lasting hundreds of seconds, or longer, have features suggesting they arise from slip-rate changes below or adjacent to seismic rupture zones. The amount of slip and its location can often be constrained by comparing data with analytic expressions for surface deformation owing to fault slip (e.g., Okada 1985).

In this review, I focus on pre-earthquake processes lasting hundreds of seconds or longer that are not detectable by short-period seismic sensors, or even necessarily by

broadband seismometers designed for frequencies as low as 0.003 Hz. I begin with brief descriptions of the capabilities of the principal instruments used to detect such pre-earthquake deformation-rate changes.

HOW WELL CAN ASEISMIC DEFORMATION BE MEASURED?

The effort to detect pre-earthquake deformation-rate changes demands high precision and long-term stability, currently unachievable with a single geodetic technique over the range from seconds to decades.

Continuous GPS (CGPS) stations, which measure absolute positions of benchmarks relative to a satellite constellation, have been widely deployed since the early 1990s (Segall & Davis 1997). White noise in CGPS position estimates has mean amplitudes of 0.5 to 4.6 mm for the horizontal components and 2.2 to 7.7 mm for the vertical component, depending on the network, the type of monument, and the data processing software (Williams et al. 2004).

Borehole strainmeters are of two main types: dilatometers, which measure volumetric expansion and contraction, and multicomponent strainmeters, which measure length changes along three or more gauges oriented at different azimuths (Agnew 1986). Both types are cemented 100 or more meters deep in specially drilled holes, and can resolve strain steps as small as a few nanostrain (10^{-9}) after filtering out strain owing to Earth tide and atmospheric pressure changes.

Long-term records from borehole strainmeters are dominated by the large strains imposed by borehole relaxation and cement curing, so these instruments cannot be used to measure absolute strain rates. They are designed for optimal performance at periods from seconds to tens of days, and special analyses are necessary to determine whether longer-duration signals are meaningful.

Creepmeters measure displacement across surface traces of faults. Only on the San Andreas Fault system in California are creepmeter data recorded at rates higher than one sample per day. Creepmeter piers are relatively shallow (2 m) in near-fault materials that can be unstable during rainfall.

Noise in every type of geodetic data increases as time periods lengthen (Johnson & Langbein 1997), generally following a power law of the form $1/f^k$, where k is between 1 and 3. Continuous GPS time series exhibit $1/f$ noise (flicker noise), although random walk ($1/f^2$) noise owing to monument instability is also believed to be present (Williams et al. 2004). Power spectra of borehole strainmeter data indicate long-period noise has frequency dependence closer to $1/f^2$.

Because noise increases with period, detection thresholds for slow deformation changes can be higher than for rapid, step-like changes. For example, in a creepmeter record, a 0.04 mm change occurring over 1 h has a signal-to-noise ratio of 2 and is therefore significant at the 95% confidence level, but a creep event occurring over 100 h needs an amplitude of 0.2 mm to attain the same significance (Langbein et al. 1993). For a borehole strainmeter exhibiting random-walk noise, a step of 3 nanostrain ramping up over 2 h may be readily detectable, but a ramp lasting 200 h must reach a level of 30 nanostrain to have the same signal-to-noise ratio (J.O. Langbein, personal

communication, 2005). Because flicker noise increases more slowly with lengthening period, CGPS sensitivity does not fall as fast with lengthening period. A practical inference is that, if a M5.5 foreshock (for example) is at the detection limit for a borehole strainmeter or CGPS station, then aseismic slip with the same moment as the M5.5 foreshock, in the same location, will also be at the limit of detection, and for the strainmeter will fall quickly below the limit as the rate of change of deformation decreases.

To unify the examples, I state approximate moments for pre-earthquake deformation, or for the amount of such deformation that could have gone undetected, as the magnitude of an earthquake having the same moment. The moment, M_0, of either seismic or aseismic fault slip, is the product of total slip, slipped area, and shear modulus (assumed here to be 3×10^{11} dyne-cm). For earthquakes, the moment magnitude, M_w, is related to M_0 by

$$M_w = (2/3)\log_{10}M_0 - 10.7, \quad (1)$$

where M_0 is expressed in dyne-cm (e.g., Shearer 1999). For some earthquakes, I have estimated the moment that could have gone undetected by comparing the coseismic deformation with the instrument's noise level, so the result is valid for pre-earthquake deformation close to the earthquake's hypocenter.

CONVERGENT MARGIN EARTHQUAKES

Changes in deformation rates prior to eight large seismic events in convergent margin settings have been detected using a wide variety of techniques.

The 1944 Tonankai (M_s8.2), 1946 Nankaido (M_w8.3), and the Anticipated Tokai Earthquakes

The recurrence of great earthquakes at intervals of 100–150 years along the Suruga-Nankai trough, off the east coast of Japan, is well-known for the past 1300 years. The most recent subduction megathrust earthquakes were the M_s8.2 Tonankai earthquake on December 7, 1944, and the M_w8.3 Nankaido earthquake on December 20, 1946 (**Figure 1**). The easternmost Tokai segment is unbroken since a M8.4 event in 1854 and is considered a dangerous seismic gap. Evidence of anomalous deformation prior to the 1944 and 1946 earthquakes has motivated the government of Japan to intensively monitor aseismic deformation, with the goal of issuing a warning prior to the next great earthquake (EERI Committee on the Anticipated Tokai Earthquake & Scawthorn 1984).

During a leveling survey near Kakegawa (**Figure 1**), approximately 40 km northeast of the 1944 Tonankai earthquake rupture zone, misclosures of 2.9 mm on one 700-m-long section were found the day before the earthquake, and misclosures of 4 mm were found on other sections a few hours before the main shock, compared with average closure errors of 0.01 mm and standard deviation of 0.024 mm. Just prior to the earthquake, the leveling bubble could not be adjusted at one measurement site; wind was ruled out as a possible cause. Sagiya (1998) examined all leveling data

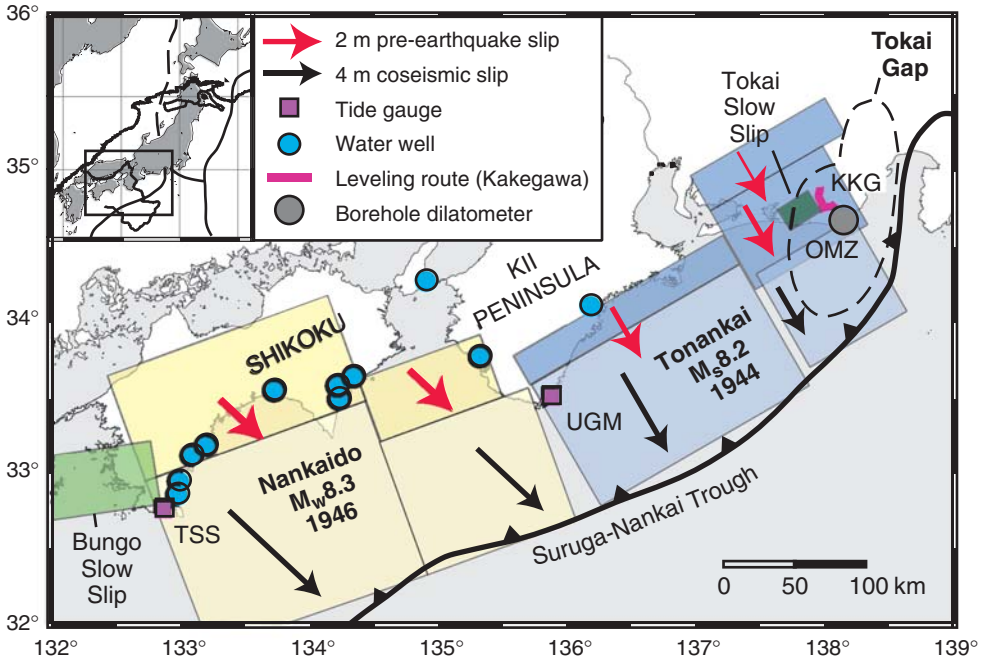

Figure 1

Map showing surface projections of rupture planes of 1944 Tonankai earthquake (*light blue*) and inferred slip planes of pre-earthquake aseismic slip (*darker blue*); rupture planes of the 1946 Nankaido earthquake (*light yellow*) and inferred slip planes of pre-earthquake aseismic slip (*darker yellow*) (Linde & Sacks 2002); inferred source area of 1997 Bungo Channel slow slip event (*light green*) (Ozawa et al. 2001); approximate source area of Tokai slow slip event (*dark green*) (Ozawa et al. 2002). Dashed line, expected rupture zone of anticipated Tokai earthquake (Ozawa et al. 2002). KKG, Kakegawa; OMZ, Omaezaki; TSS, Tosashimizu; UGM, Uragami.

collected by that crew for a month-long period spanning the Tonankai earthquake, and judged it reliable, although he did identify one additional unexplained large closure error. The large closure errors, all consistent with preseismic north-down tilt, were observed on consecutive sections of the routes. Closure errors of opposite sense occurred in the days following the Tonankai earthquake.

There is also evidence of deformation prior to the 1946 Nankaido earthquake. Tide-gauge records from Tosashimizu (**Figure 1**) indicate the ground there rose 10 cm within a few days before the earthquake, although no postearthquake elevation changes took place at this site (Sato 1982). The tide gauge at Uragami indicated subsidence of 10–20 cm before the Nankaido earthquake (Kobayashi et al. 2002). In addition, water-level drops in wells, drying of wells, and muddying of well water (**Figure 1**) were reported, consistent with either extensional strain or uplift.

The opposite signs of the pre- and postseismic tilts for the 1944 Tonankai earthquake are consistent with preseismic slip deeper than the seismic rupture. Linde & Sacks (2002) showed that all the observed deformation, for both earthquakes, could

be explained assuming 2-m aseismic slip of the subduction interface downdip of each respective seismic rupture at depths below 25 km (**Figure 1**). The preseismic slip moment was about one fourth the moment of each mainshock, which entailed seismic slip of 4 to 6 m.

Crustal deformation instrumentation in the Tokai area now includes dilatometers, tiltmeters, CGPS, and fluid pressure sensors. Linde & Sacks (2002) show that if the anticipated Tokai earthquake is preceded by 2 m of slip downdip of the rupture area, peak signals of several microstrain (10^{-6}) are expected at each of five dilatometers. This signal would be well above the noise level if it should occur over a period of days.

In 1994, the Geographical Survey Institute of Japan brought the GEONET (GPS Earth Observation Network) online (see **http://mekira.gsi.go.jp/**), which currently consists of about 1200 CGPS stations. GEONET has revealed transient aseismic slip on the subduction interface of the Suruga-Nankai trough. Beginning shortly after the December 3, 1996 M_w 6.7 Hyuganada earthquake, CGPS stations near the Bungo Channel, Japan, recorded displacement-rate changes lasting about one year (**Figure 1**). Ozawa et al. (2001) inverted displacements at 15 CGPS stations to show that 50–200 mm of slip apparently occurred on a west-dipping surface extending to 50 km depth, just above the Phillippine Sea plate. This slip surface abuts the western edge of the rupture zone and hypothesized preseismic slip zone of the 1946 Nankaido earthquake (**Figure 1**).

Ozawa et al. (2002) reported that displacement rates measured by GEONET stations in the Tokai area changed beginning in October 2000, with southeastward motion of about 20 mm at four stations as of June 2002, and southward movement and uplift continuing through 2004 (CCEP 2005). They modeled the displacements as originating from aseismic slip on the subduction interface at the western end of the anticipated Tokai earthquake source region (**Figure 1**), near the location inferred by Linde & Sacks (2002) for slow slip preceding the 1944 Tonankai earthquake. Takano et al. (2003) describe leveling and tide-gauge evidence for a slow slip event in the same area in 1988. Ozawa et al. (2002) argue that the recent slip events corroborate the occurrence of aseismic slip before the 1944 Tonankai earthquake, and point out that the slow slip event is increasing stress favoring failure of the Tokai segment.

Kuroki et al. (2004) created a three-dimensional numerical simulation of the Tokai subduction interface to investigate the conditions under which slow slip events would occur between great earthquakes. Their model assumed rate- and state-dependent friction, with a long characteristic slip distance, L (5 cm), and $L = 15$ cm in the depth range of the slow slip events (22–27 km). Five slow slip events occur during each 450-year simulated earthquake cycle, beginning 200 years after the last simulated large earthquake. Several years into the fifth slow slip event, preslip initiates near the impending earthquake hypocenter, which is shallower (16 km depth) than the slow slip events. Slow slip events arose only for L larger over at least a 3 km depth range, and were followed by earthquakes only for curved plate interfaces. They infer that curvature can focus the enhanced stress caused by the slow slip event, enabling that stress to trigger seismic rupture. The model simulates GPS-observed displacement directions well, but the simulated slow slip events last longer than observed events.

Preslip develops in less than one day, but might be detectable by a dilatometer at Omaezaki (**Figure 1**), where contractional strain of 10 nanostrain is simulated in the hours before the earthquake.

The May 26, 1983, Japan Sea Earthquake (M_s7.8)

Mogi (1985) describes accelerating coastal uplift during the six years prior to this reverse-faulting earthquake, which ruptured a poorly defined convergent boundary at the eastern edge of the Japan Sea (**Figure 2**). Leveling surveys indicated 2 cm uplift on the Oga peninsula during the periods 1969–1977 and 1977–1981, and 4 cm uplift on the Fukaura peninsula between 1975 and 1981. Tide-gauge readings at Oga and Fukaura confirmed the uplift, although a water-tube tiltmeter on the Oga peninsula recorded tilt of opposite sign. The uplift at Fukaura was attributed to an unusual earthquake swarm at Iwasaki in September 1978, but recognition of the uplift as anomalous prompted the Coordinating Committee for Earthquake Prediction (CCEP) to meet in February 1982. The CCEP did not reach a "concrete conclusion" about possible impending seismic events, but at its recommendation, three borehole strainmeters were installed in October–December 1982 (**Figure 2**). The strainmeter closest to the coast, GJM, recorded 86 anomalous strain events, with amplitudes of 10–30 nanostrain and durations of about 3 h, in the 6 months remaining before the mainshock (Linde et al. 1988).

Figure 2

Map showing rupture planes of the 1983 Japan Sea earthquake, inferred slip planes of pre-earthquake aseismic slip, and leveling routes (modified from Iio et al. 2002), viewed by some as the border between the Amurian and North American plates (see Seno & Sakurai 1996 for alternative views of plate boundaries in this region).

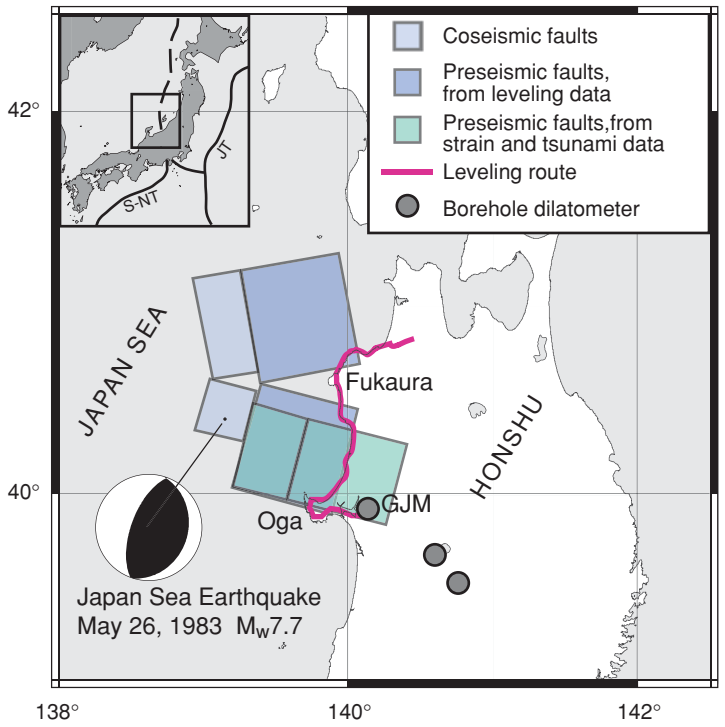

On May 26, 1983, the Japan Sea earthquake occurred 50 km offshore. None of the continuously operating tide gauges, strainmeters, or tiltmeters recorded immediate pre-earthquake accelerating deformation, although foreshocks (some $M > 5$) occurred 6–12 days prior to the mainshock, near the hypocenter (Mogi 1985). Post-earthquake leveling revealed the previously uplifted peninsulas had subsided, and the aseismic strain events stopped after the major aftershocks, consistent with the uplift and strain events being related to the impending earthquake.

Mogi (1985) cites studies attributing the pre-earthquake deformation to slip downdip of the seismic rupture zone. Iio et al. (2002) quantified this idea in a possible model for the preseismic deformation, entailing 5.7 m total preseismic slip on downdip extensions of the coseismic rupture planes (**Figure 2**), 4 m of this (about half the coseismic slip) within a few minutes prior to the earthquake. Iio et al. (2002) further proposed that slip accelerated from 25 mm/year, 7.8 years prior to the earthquake, to 10 mm/s in the last few minutes before the earthquake, based on the time sequence of leveling and strain observations, as well as tsunami modeling.

Accelerated slip in a several-year period prior to the 1982 M_s6.8 Urakawa-oki, Japan, earthquake, detected by leveling, is also described in Iio et al. (2002).

The May 22, 1960, Chile Earthquake (M_w9.2)

Kanamori & Cipar (1974) and Kanamori & Anderson (1975) first suggested that a slow precursor preceded the May 22, 1960, M_w9.2 Chile earthquake, in which interplate slip of 20–30 m took place throughout a rupture zone 920 $\pm$ 100 km long. A 33-h foreshock sequence occurred north of the mainshock, with seismic activity propagating toward the mainshock hypocenter at a speed of 1 m s^{-1} (86 km day^{-1}; Cifuentes 1989). Cifuentes & Silver (1989) digitized records from long-period seismometers, utilizing data in the 1–5 mHz frequency band. Spectrograms of these data exhibit a scalloped pattern, with holes in the amplitude spectra at relatively long periods. Such holes are absent from recordings of the 1985 Central Chile earthquake, 550 km N of the 1960 rupture initiation point, ruling out path effects as the cause. Cifuentes & Silver (1989) modeled these features of the data by assuming preseismic and afterslip events in addition to the mainshock, with the preseismic slip beginning 20 min prior to the mainshock, having a rise time of 5 min and moment almost two thirds that of the mainshock. The scalloped pattern and spectral amplitude holes result from interference of the preseismic slip, the mainshock, and a postseismic event 6 min after the mainshock. The data can also be explained without the afterslip, in which case the best-fitting preseismic event begins 14 min before the mainshock and has one-third of the mainshock moment. Kanamori & Cipar (1974) argued that the coastal uplift data required interplate slip extending deeper than the mainshock seismic rupture. Linde & Silver (1989) showed that coastal uplift from 1960 to 1968 required slip over a zone with downdip width at least 300 km (i.e., to a depth between 65 and 80 km). Because the seismic rupture was constrained to a downdip width of 140 km, and earthquakes do not occur deeper than 30 km, Linde & Silver (1989) also concluded that the uplift data require slip deeper than the mainshock seismic rupture.

However, the uplift data do not preclude this slip occurring after, rather than before, the mainshock.

Aseismic slip before the 1960 Chile earthquake probably took place either downdip of the seismic rupture zone and/or to the north where the foreshock sequence occurred. However, the long-period teleseismic data used to identify the 15-min slow precursor have poor spatial resolution and cannot rule out the possibility that the slow precursor represented accelerating slip over the seismic rupture area.

Since long-period seismic data are now collected routinely, an obvious question is whether slow precursors precede other earthquakes. Ihmlé & Jordan (1994) found 20 events with slow precursors (all but one on oceanic transform faults; see Oceanic Transform Faults, p. 617) among 107 shallow-focus earthquakes, but of the 23 events in plate convergence zones that they studied, none required a slow precursor to model the low-frequency waveforms. Other studies (e.g., Okal & Newman 2001) have shown that some subduction zone earthquakes have slow source-time functions, but not necessarily slow beginnings. During the M_w9.1 December 26, 2004, Sumatra-Andaman earthquake, rupture apparently slowed from 2.8 to 2.1 km s^{-1} after propagating along 450 km of its 1200-km-long rupture zone (Tolstoy & Bohnenstiehl 2005).

The March 28, 1964, Prince William Sound, Alaska, Earthquake (M_w9.2)

The history of coastal elevation relative to sea level at four sites in Alaska, inland from the seismic rupture zone of the 1964 Prince William Sound earthquake, has been found to include not only interseismic relative sea level drop and coseismic submergence, but also periods of relative sea level increase prior to the 1964 earthquake (Shennan et al. 1999; Zong et al. 2003; Hamilton & Shennan 2005a,b).

Relative sea level histories are reconstructed from microfossil assemblages (diatoms, foraminifera, pollen, and thecamoebians), ranging from fully marine to salt-intolerant, in coastal sediment cores. For example, Shennan et al. (1999) describe a 28-cm core from Girdwood Flats, on the coast of the Turnagain Arm of Cook Inlet (**Figure 3**). Samples from depths of 26 to 13 cm indicate falling relative sea level, consistent with interseismic uplift. The 1964 coseismic subsidence (1.7 m) is reflected in the peat-to-silt contact 10 cm below the surface, as well as by a change in biofacies zones. Samples from 11–12 cm below the surface contain biofacies indicative of rising relative sea level.

The evidence for pre-earthquake relative sea level rise has since been strengthened by using ^{137}Cs dating to show that relative sea level rise started near the 1952 horizon (Zong et al. 2003) and by expanding the study to four sites. By studying peat-silt contacts corresponding to earlier great earthquakes, pre-earthquake relative sea level rise averaging 0.12 ± 0.13 m was shown to have occurred before the 1964 earthquake, as well as before an earlier event 850 years ago (Hamilton & Shennan 2005a,b).

The highest estimates of changes in coastal uplift rate are approximately 10 mm/year, detectable in tide-gauge records. Unfortunately, the only tide-gauge data within 100 km of the microfossil sites prior to the 1964 earthquake are annual averages from Seward (**Figure 3**), which contain a large amount of scatter (Savage & Plafker

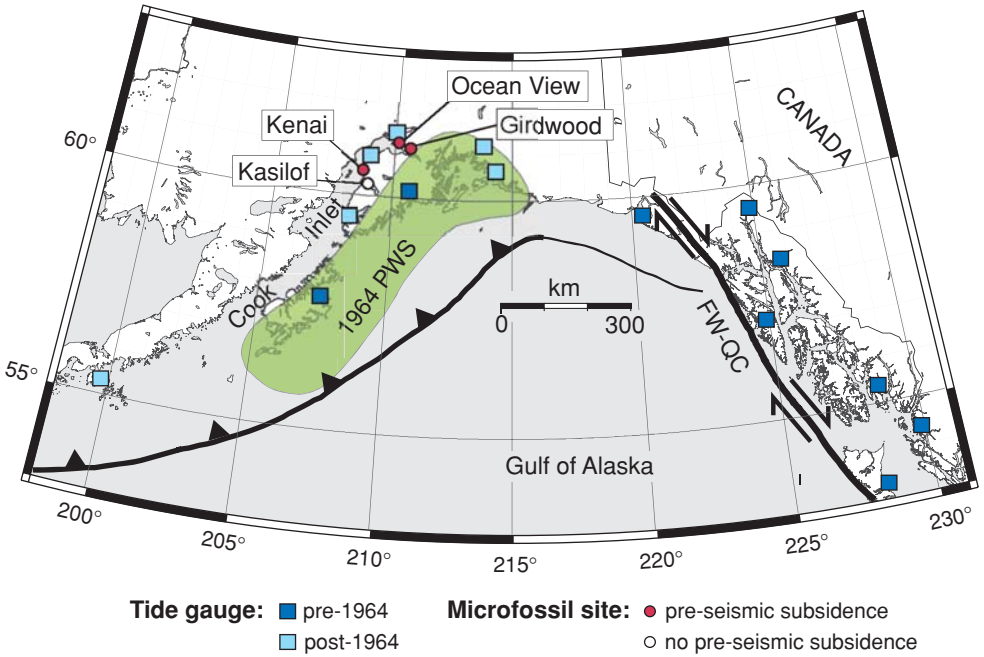

Figure 3

Map showing locations of microfossil studies of relative sea level history in southern Alaska (Long & Shennan 1994, Shennan et al. 1999, Zong et al. 2003). Also shown are tide-gauge locations, the rupture area of the 1964 Prince William Sound earthquake (*green*), and tectonic boundaries in southern Alaska (modified from Larsen et al. 2003).

1991). Larsen et al. (2003) analyzed monthly average tide-gauge records from coastal Alaska from 1937 to 2001; distant tide gauges installed before the 1964 earthquake show no evidence of a secular trend change between 1952 and 1964.

The Cook Inlet area experienced several earthquakes above M5.7 between 1952 and 1964, with the largest event being an intraplate M_w6.7 strike-slip earthquake 50–60 km deep, 70 km southeast of Girdwood Flats in October, 1954 (Doser & Brown 2001). Since 1964, no earthquakes above M5 have occurred beneath the central or southern Kenai Peninsula, suggesting the pre-1964 seismicity was related to the impending earthquake.

The 1700 Cascadia Earthquake (M9)

The occurrence in 1700 of a great (M9) subduction interplate earthquake along the Pacific coast of Oregon and Washington, and Vancouver Island, Canada (Cascadia), is known from paleoseismic, tsunami, and microfossil studies (Hemphill-Haley 1995, Atwater 1996, Nelson et al. 1996, Satake et al. 1996). Microfossils in cores from Netarts Bay, coastal Oregon (**Figure 4**), yield evidence for rising relative sea level preceding the coseismic subsidence (Shennan et al. 1998). Shennan et al. (1996) had

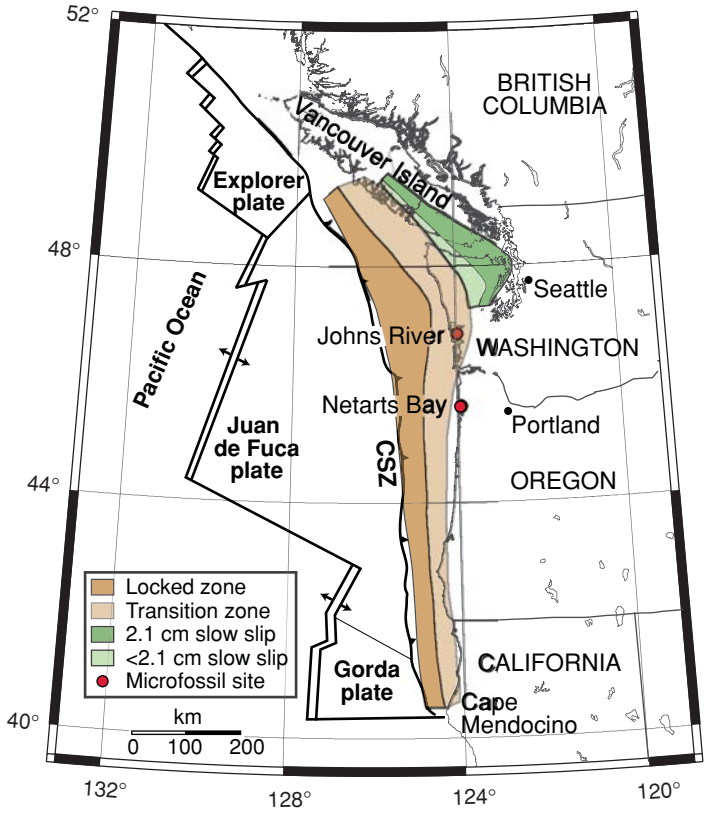

Figure 4

Map showing locations of microfossil studies of relative sea level history in Oregon and Washington (Shennan et al. 1996, 1998). CSZ, seaward limit of Cascadia subduction zone. Green shading is inferred area of slow slip event in August 1999 (Dragert et al. 2001).

previously found evidence for preseismic rising relative sea level for horizons corresponding to submergence events (presumably paleoearthquakes) around 5000 and 3600 years ago in peat-mud couplets from Johns River in southwestern Washington. For the more recent submergence events, they found no evidence at Johns River for preseismic relative sea level rise. As for the Alaska studies, the preseismic deformation was in the same sense as the coseismic deformation, but timescales of possible preseismic sea level rises could not be determined for Cascadia.

As in Japan, intensified CGPS monitoring in Cascadia has revealed transient slip episodes on the subduction interface. Dragert et al. (2001) first reported an aseismic event displacing CGPS stations in northwest Washington and southern Vancouver Island 2–4 mm in the direction opposite to usual plate motion (**Figure 4**). Miller et al. (2002) showed that such events recur at average intervals of 14 months, lasting about two weeks. Aseismic subduction with total offset of 20–40 mm in the depth range 25–40 km, downdip of the inferred locked seismogenic zone, can account for the observed CGPS displacements during these events. Rogers & Dragert (2003) showed that the aseismic slip is accompanied by seismic tremor originating above the slip source. These short-duration slip events produce primarily horizontal motion at the surface, so similar events cannot explain the preseismic relative sea level increases

found in microfossil studies. Although no great earthquake has followed any of the episodic slip events to date, Mazzotti & Adams (2004) point out that two-thirds of total plate convergence during each 14-month period takes place during the slip events, possibly elevating the probability of a great earthquake 30 to 100 times above background at those times.

The July 7, 2001, Peru Earthquake (M_w7.6 Aftershock of M_w8.4 Mainshock)

Melbourne & Webb (2002) analyzed CGPS data from station AREQ, located approximately 300 km inland from the epicenter of the M_w8.4 Peru earthquake on June 23, 2001 (**Figure 5**). Horizontal coseismic displacements up to 50 cm accompanied the M_w8.4 mainshock, but no pre-earthquake deformation was observed. However, during postseismic movement of about 1 cm per week, deformation accelerated for 18 h prior to the largest (M_w7.6) aftershock on July 7, approximately 200 km from AREQ. The deformation before the M_w7.6 aftershock, which totaled 2.0 $\pm$ 0.5 cm in the south direction and less in the west direction, is unique in three years of data, and was terminated by the aftershock. Presuming slip during the 18 h prior to the July 7 earthquake was parallel to plate convergence, and occurred on the Nazca plate interface, then the AREQ data are best modeled by slip near the aftershock, suggesting that the aftershock and accelerated slip were related.

It is estimated that the moment of the preseismic accelerated slip was about twice that of the aftershock, which produced no coseismic offset in the AREQ time series. Therefore, the preseismic acceleration probably represents slip over a larger area than the aftershock, rather than an acceleration of slip over the aftershock rupture plane.

This data set illustrates that even with careful filtering, CGPS is unable to resolve the coseismic displacement from a M7.6 earthquake at a distance of 200 km, and would therefore not be expected to detect aseismic slip of equivalent moment at this distance.

The Sept. 25, 2003, Tokachi-oki Earthquake (M_w8.3): No Preseismic Deformation Rate Change Detected

The September 25, 2003, Tokachi-oki earthquake was the first subduction megathrust earthquake on the Japan coast since the GEONET CGPS network came online in 1994. Irwan et al. (2004) analyzed 1-Hz GPS data for 14 stations 70–240 km from the epicenter, finding coseismic displacements as large as 1 m. One to two meters of coseismic slip was inferred on the downdip portion of the coseismic rupture plane, which extends directly below three of the GEONET stations at a depth of about 30 km (Miura et al. 2004). During the 30 min preceding the mainshock, the 1-Hz data from the closest station exhibit fluctuations of 1–2 cm in the horizontal components and up to 5 cm in the vertical component, with no preseismic deformation-rate change distinguishable from these background variations. Background variations in 30-s data from the same station during the 20 h prior to the mainshock are of similar size for the horizontal components, but as large as 10 cm for the vertical component. Again,

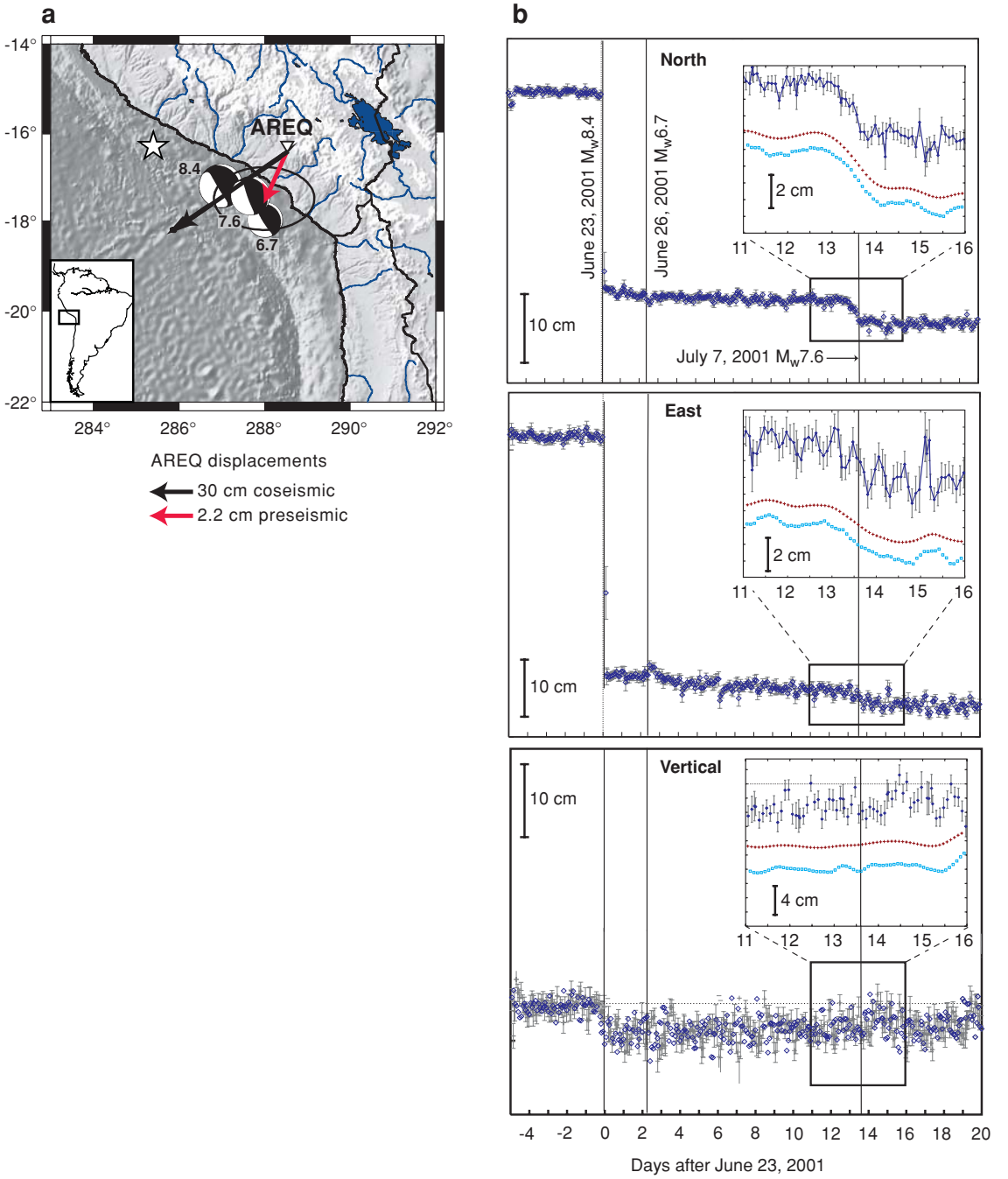

no preseismic deformation is discernible above this background. These observations constrain the moment of preseismic slip on the rupture plane, in this time frame, to be less than 1% of the mainshock moment, equivalent to a M7 earthquake.

Summary of Observations for Convergent Margins

Credible studies indicate pre-earthquake aseismic deformation-rate changes occurred before eight earthquakes in convergent margin settings, six with $M > 8$, one M_w7.6 aftershock of a larger subduction earthquake, and one M7.2 event. Six separate techniques were used to observe these quantities, and more than one type of instrument recorded the preseismic deformation only for the 1946 Nankaido (tide gauges and groundwater level) and 1983 Japan Sea (leveling, tide gauges, and borehole strain) earthquakes.

Deformation rate changes prior to the 1944 Tonankai, 1946 Nankaido, 1983 Japan Sea, and 1982 Urakawa-oki earthquakes are consistent with slow slip downdip of the area that ruptured seismically. Accelerated deformation prior to the 2001 Peru M_w7.6 aftershock also probably took place off of the aftershock rupture area, although within the mainshock rupture zone. The slow precursor to the 1960 Chile earthquake could have occurred downdip or along strike; like many earthquakes examined by Perez & Scholz (1997), foreshocks to the 1960 Chile earthquake took place at one end of the rupture zone. However, nearfield CGPS data show that no comparable downdip slip preceded the 2003 M_w8.3 Tokachi-oki earthquake during the same pre-earthquake interval.

Subduction zones have a higher rate of foreshock activity than other tectonic settings (Reasenberg 1999), but of the examples summarized here (excluding the 2003 Peru aftershock and the 1700 Cascadia earthquake), foreshocks occurred on the timescale of preseismic deformation only for the 1960 Chile, 1983 Japan Sea, and possibly the 1964 Alaska earthquakes. Crustal deformation unaccompanied by foreshocks may support the source of the pre-earthquake deformation being deeper than the brittle seismogenic zone. Recent CGPS detection of aseismic transient slip events in the Japan and Cascadia subduction zones show that transient aseismic slip does occur, and is likely to influence the loading path of subduction interfaces to

Figure 5

(*a*) Measured GPS offsets during the June 23, 2001, M_w8.4 Peru mainshock and aftershocks. Black vector shows coseismic displacements owing to the mainshock, red vector denotes measured preseismic offset prior to the July 7, 2001, M_w7.6 aftershock. Error ellipses are 2 standard deviations. White star shows National Earthquake Information Center rupture nucleation site for M_w8.4 mainshock. Triangle denotes position of CGPS station AREQ at Arequipa, Peru. (*b*) Coseismic deformation recorded at AREQ from the mainshock and two major aftershocks. Vertical lines denote times of major aftershocks. Filtered data (insets) are computed with an acausal $n = 3$ symmetric smoothing window (*red crosses*), and a causal, single-pass Butterworth filter with a 12-h corner (*light blue squares*) (modified from Melbourne & Webb 2002).

failure, although the aseismic slip events observed with CGPS to date have not been followed by great earthquakes.

TERRESTRIAL EARTHQUAKES

Earthquakes on well-monitored terrestrial faults are generally lower magnitude than subduction zone events. However, they are also in many cases shallower, and, in principle, able to be more completely monitored by geodetic instrumentation.

The 1985 Kettleman Hills, California, Earthquake (M_w6.1)

Small relative water level rises were recorded in two of four wells monitored near Parkfield, California, starting three days prior to the August 4, 1985, M_w6.1 Kettleman Hills earthquake (**Figure 6**; Roeloffs & Quilty 1997). A contractional pre-earthquake strain transient of similar duration was recorded on two borehole dilatometers about 150 m from the Gold Hill well; one other newly installed borehole strainmeter near Parkfield did not record a pre-earthquake strain change. The Kettleman Hills earthquake represented blind thrust faulting on a fault subparallel to and about 35 km northwest of the San Andreas Fault in central California. It was preceded by a M4.1 foreshock 22 h prior to the mainshock and a M4.7 foreshock 30 min prior to the mainshock in the immediate vicinity of the hypocenter (Ekström et al. 1992). Water level dropped in all four wells monitored at the time of the Kettleman Hills earthquake on August 4, and all three strainmeters recorded coseismic crustal expansion.

The groundwater-level changes can be expressed in units of strain based on the wells' responses to Earth tides. When this is done, the water-level and dilatometer data are consistent with extensional coseismic strain of 0.05 to 0.1 microstrain, preceded by contractional strain equal in magnitude but opposite in sign.

In the Joaquin Canyon well, the 3-cm water-level rise preceding the Kettleman Hills earthquake remained one of only two unexplained signals this large from 1985 through 1996. Signals comparable in size to the pre-earthquake variation were recorded frequently in the Gold Hill well, however. Roeloffs & Quilty (1997) showed that one of the two wells in which no pre-earthquake changes were observed taps a poorly confined aquifer, in which equilibration with the water table suppresses water level changes in response to strain that varies slowly in time. The International Association for Seismology and Physics of the Earth's Interior (IASPEI) Sub-Commission on Earthquake Prediction (Wyss & Booth 1997) reviewed the Kettleman Hills observations and added them to their Preliminary List of Significant Precursors in 1994. High-frequency dilatometer recordings constrain the moment of preseismic slip in the minutes to seconds prior to the Kettleman Hills mainshock to a small fraction of the mainshock moment (Johnston et al. 1987), but do not rule out pre-earthquake deformation on a three-day timescale.

Because the pre-earthquake water level and strain changes were opposite in sign to coseismic changes, if they were caused by aseismic slip in the same sense as the Kettleman Hills earthquake, that slip must have taken place on a part of the fault plane complementary to the mainshock rupture. A nonunique model that accounts

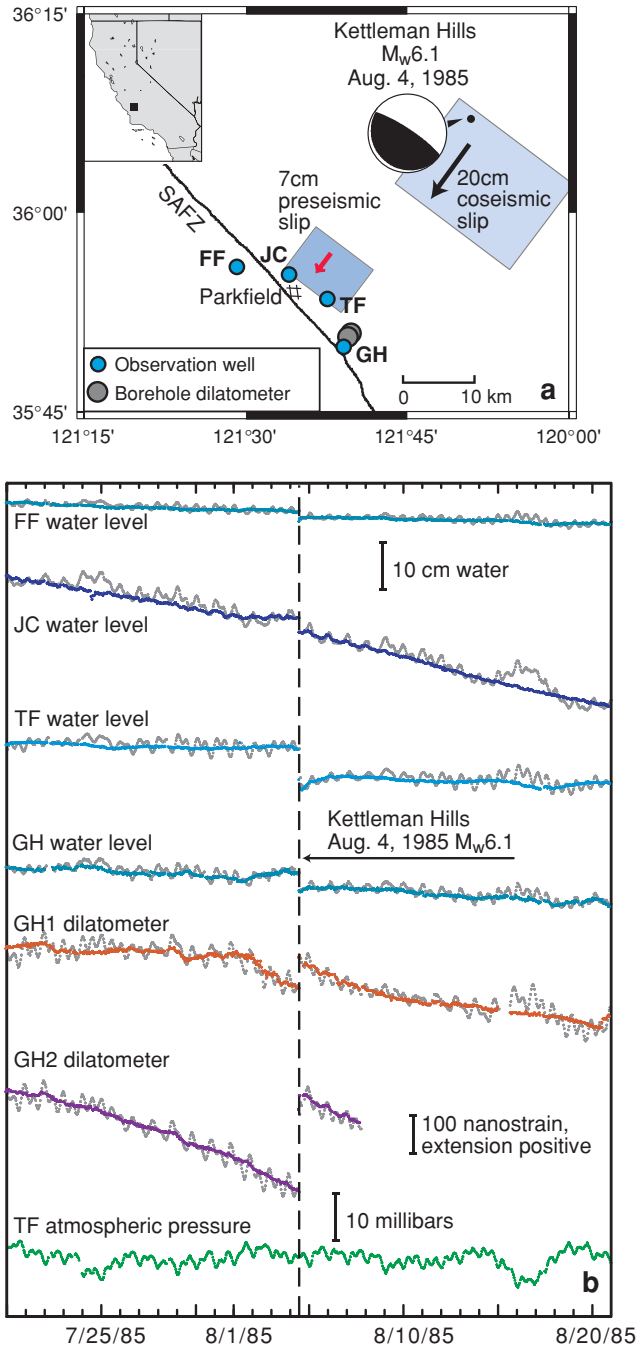

Figure 6

(*a*) Map showing location of 1985 M_w6.1 Kettleman Hills, California, earthquake, groundwater level observation wells, and borehole dilatometers operating near the town of Parkfield at that time. SAFZ, San Andreas Fault zone. Arrows give directions of preseismic and coseismic movement of foot wall relative to hanging wall. (*b*) Groundwater level, dilatometer, and atmospheric pressure data for August 1985. Data shown in gray are raw observations, and colored curves show data after removal of earth tide- and barometric pressure–induced fluctuations.

for the pre-earthquake changes is slip of 7 cm over a 10 km × 7.5 km low-angle thrust at the depth of the downdip end of the earthquake rupture (**Figure 6*a***).

The largest earthquake in the Kettleman Hills area since the 1985 M_w6.1 event was of M5.3 on February 14, 1987; no coseismic or preseismic water level or strain changes were associated with that event. A M4.7 event near Parkfield on December 20, 1994, produced coseismic water level changes in two wells, but no pre-earthquake water level or strain changes were observed (Quilty & Roeloffs 1997).

The 1989 Loma Prieta, California, Earthquake (M_w6.9): No Preseismic Deformation Rate Change Detected

The October 18, 1989, Loma Prieta earthquake broke a 70°-dipping fault southwest of the San Andreas Fault (e.g., Wald et al. 1991). It was preceded by two earthquakes now widely regarded as foreshocks: the June 27, 1988, M5.3 (LE1) and August 8, 1989, M5.4 (LE2) Lake Elsman earthquakes (**Figure 7*a***). However, reported changes in deformation rates prior to the Loma Prieta earthquake no longer appear significant after further analysis.

Lengths of three lines in the epicentral area had been monitored monthly since 1981 using a geodolite (**Figure 7*a***); the standard deviation of these measurements was 7–9 mm. Campaign-type GPS measurements of the same lines began in 1987 (Lisowski et al. 1993). Lisowski et al. (1990) reported changes in the shortening rates of the two lines that do not cross the San Andreas Fault, but on later analysis these changes were judged indistinguishable from background variations (Lisowski et al. 1993). The third geodolite line (Eagle Rock, 31.4 km long) crossed the Loma Prieta rupture zone between the epicenters of the two Lake Elsman foreshocks. No significant change in the shortening rate of this line was observed between 1986 and the Loma Prieta earthquake. Strain changes smaller than 0.28 microstrain would not have been detectable by the geodolite surveys; for the GPS data, strain exceeding 0.17 microstrain might have been detected.

Two borehole strainmeters operated by the U.S. Geological Survey (USGS) near the San Andreas Fault, approximately 40 km south of the Loma Prieta epicenter (**Figure 7*a***), recorded strain rate changes prior to the earthquake, but in the context of the much longer records now available, these changes no longer appear unusual. Gladwin et al. (1991) reported that the three-component borehole strainmeter near San Juan Bautista recorded faster fault-parallel shear strain for a year before the earthquake, totaling about 1 microstrain, approximately 30% of the coseismic strain step. The dilatometer apparently recorded a change in strain rate beginning in mid-1988 (Johnston et al. 1990, Johnston & Linde 1993). A preliminary report that the amplitude of Earth-tide-induced strain in the dilatometer data changed prior to the Loma Prieta earthquake was later shown to be an instrumental artifact (Linde et al. 1993).

The year-long strain rate change reported by Gladwin et al. (1991) can be revisited now with 15 more years of data. **Figure 7*b*** shows raw data from the SJB three-component borehole strainmeter for the period from 1984 until May 2005. The strain rate changes prior to the Loma Prieta earthquake are discernible only after removing

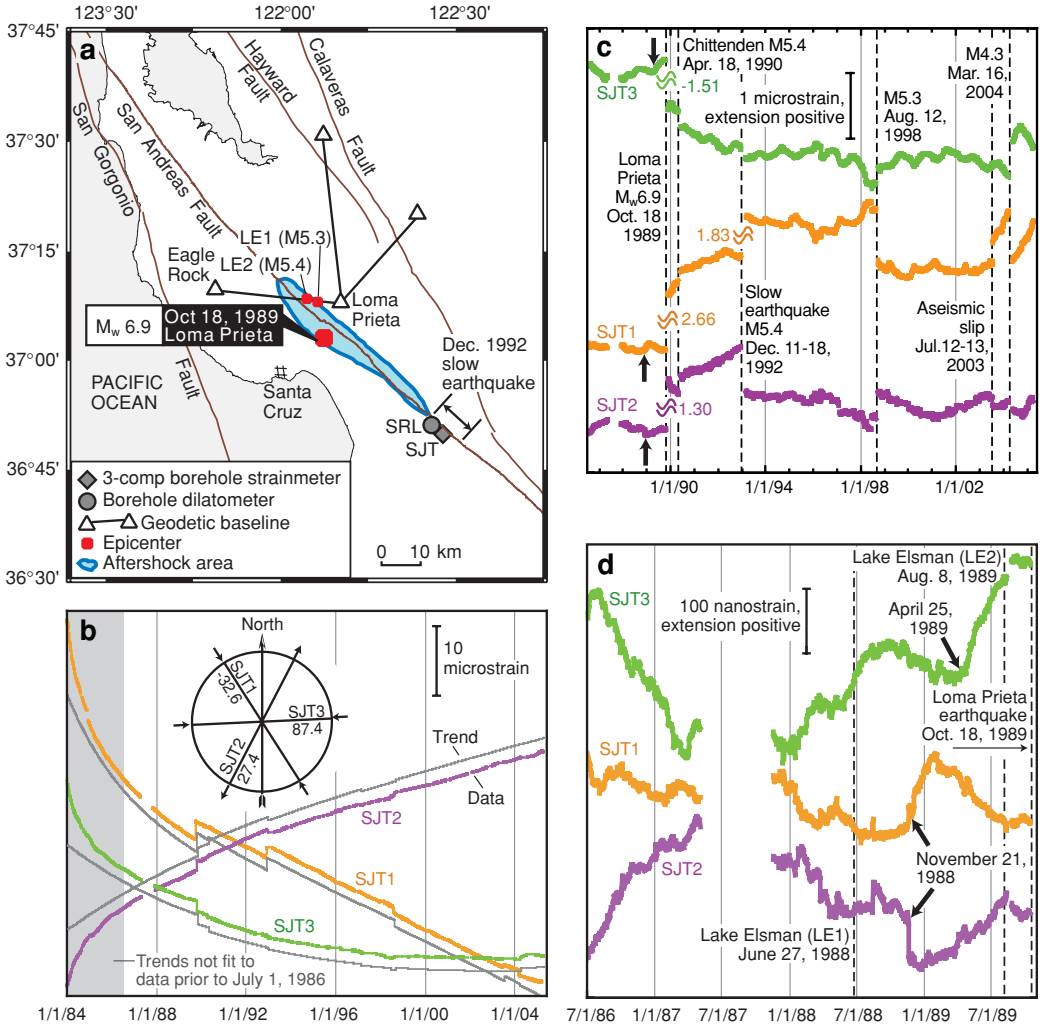

Figure 7

(*a*) Map showing location of Oct. 18, 1989, M_w6.9 Loma Prieta, California, earthquake, borehole strain instrumentation; geodetic baselines; and location of slow earthquake in December 1992. (*b*) Daily averages of data from individual gauges of the SJT 3-component borehole strainmeter (*colored*); trends (exponential + quadratic + linear) and step offsets fit to the data (*gray*). Inset shows gauge orientations. Each gauge records a weighted sum of areal strain and linear strain along the gauge azimuth, as described in Gladwin et al. (1991). Data from USGS, in cooperation with University of Queensland and Commonwealth Scientific and Research Organization, Australia. (*c*) Eighteen-minute gauge data from SJT after subtracting the trends shown in (*b*). Large offsets owing to earthquakes and aseismic strain events have been compressed and labeled with total offset in microstrain. Bold arrows show beginnings of strain rate changes described as possible precursors to the 1989 Loma Prieta earthquake. (*d*) Same data as in (*c*), for the period prior to the Loma Prieta earthquake. Bold arrows indicate initiation times of strain rate changes prior to the earthquake.

the strong trends owing to borehole relaxation and grout curing (**Figure 7*b***). **Figure 7*c*** shows the original data after subtracting estimated trends; it is evident that strain rate changes similar to those preceding the Loma Prieta earthquake occur at many other times. Although the strain rate changes could still be related to the Loma Prieta earthquake, they are not readily distinguishable from background variations.

In **Figure 7*d***, the rate changes prior to the Loma Prieta earthquake on gauges 1 and 2 can be seen to initiate with abrupt steps on November 21, 1988. These steps are one of a series of strain events that continued after the Loma Prieta earthquake [see San Juan Bautista, California: Small ($M < 3.7$) Earthquakes Embedded in an Aseismic Slip Episode, December 1992, below; Gladwin et al. 1994]. On gauge 3, the rate change seems to begin later, around April 25, 1989.

The Lake Elsman foreshocks suggest a year-long preparation period preceded the Loma Prieta earthquake. However, coseismic strain from both Lake Elsman events is below background fluctuations recorded by the San Juan Bautista strainmeter 40 km away (**Figure 7*d***), and barely resolvable using trilateration measurements of a 31-km-long line passing directly above the hypocenters. These negative observations imply aseismic slip with moment equivalent to a M5.4 earthquake near the Loma Prieta mainshock hypocenter could have escaped detection by instrumentation operating at that time.

The 1992 Landers (M_w7.3) and 1999 Hector Mine (M_w7.1), California, Earthquakes: No Preseismic Deformation Rate Change Detected

The June 28, 1992, M_w7.3 Landers earthquake, in the eastern California shear zone, was preceded by 30 foreshocks (maximum magnitude of M_L3.7) in the 6.6 h prior to the mainshock (Dodge et al. 1996, Hauksson et al. 1993). M_w4.4 and M_w5.6 subevents in the 3 s prior to the main energy release initiated the rupture (Abercrombie & Mori 1994). Dodge et al. (1996) showed that the foreshocks imposed cumulative stress and fluid pressure changes at the mainshock hypocenter that should have stabilized, not loaded, the fault, and they concluded the foreshocks were incidental to a largely aseismic nucleation process.

The nearest crustal deformation measurements to the Landers mainshock were CGPS stations, strainmeters, and tiltmeters at Piñon Flat (68 km S of the epicenter; Wyatt et al. 1994) and a borehole dilatometer at Devil's Punchbowl (100 km W of the Landers rupture, 135 km NW of the epicenter; Johnston et al. 1994). Ten-minute and 4-s data from the dilatometer show no pre-earthquake strain rate changes. None of the instruments at Piñon Flat indicated preseismic changes in the 300 s prior to the mainshock. In particular, the lack of signal on the laser strainmeter constrains the moment of preseismic slip near the mainshock hypocenter to less than that of a M_w4.8 earthquake.

The only anomalous feature of crustal deformation rates preceding the Landers earthquake was that strain rates changed, as recorded by a borehole strainmeter and several long-base laser strain components at Piñon Flat, following the coseismic step

from the April 23, 1992, Joshua Tree earthquake (M_w6.1), now regarded as an early Landers foreshock (Wyatt et al. 1994).

The October 16, 1999, Hector Mine earthquake, which ruptured faults passing within 20 km east of the Landers rupture, is widely believed to have been stimulated by the Landers event less than 8 years earlier. For example, a July 1992 Landers aftershock took place about 3 km west of the future Hector Mine epicenter, in a previously aseismic area (Hauksson et al. 2002). The Hector Mine earthquake was preceded by 18 foreshocks (maximum magnitude 3.7) beginning 19 h prior to the mainshock, and within 1 km of the mainshock epicenter. Despite indications for an extended preparation period, little or no evidence exists of deformation rate changes prior to the Hector Mine mainshock.

The six CGPS stations installed between the Landers and Hector Mine ruptures between October 3, 1998, and September 2, 1999, could have missed pre-earthquake slip near the Hector Mine hypocenter with moment as large as a M_w6.4 earthquake. The closest station, LDES, is about 25 km from the Hector Mine surface rupture, and the others are within 60 km. Coseismic displacements at LDES were 17 cm N, 7 cm W, and 2 cm up (see **http://sideshow.jpl.nasa.gov/mbh/all/LDES.html**). Error bars on daily positions are about 2 cm horizontal and 4 cm vertical; seasonal and other variations are about twice that.

Mellors et al. (2002) used interferometric synthetic aperture radar (InSAR) to search for aseismic slip during the 30 days prior to the Hector Mine earthquake, detecting none. Synthetic noise studies indicated slip with moment equivalent to a M4.5 earthquake at a depth of 5 km would be just resolvable with InSAR. However, they were unable to resolve coseismic displacement from a nearby M_L5.4 event at 9.6 km (or shallower) depth in 1992, suggesting that the detection threshold could be higher for noise characteristics of real data. InSAR techniques are evolving, and it has been shown that, using permanent scatterers, surface fault movements can be detected in areas with sparse vegetation (Lyons & Sandwell 2003).

Using campaign GPS data, Austin & Miller (2002) found pre–Hector Mine velocities (1993–1998) discordant with the overall velocity field of the Mojave region, attributing the discordant velocities to post-Landers loading. Hector Mine coseismic displacement at these sites agreed in direction with these discordant velocity vectors, suggesting the post-Landers loading promoted the Hector Mine rupture. This is one of few examples where geodetic data have been invoked to support postearthquake stress transfer calculations. No acceleration prior to the Hector Mine earthquake was detectable with campaign GPS data; instead it was necessary to identify stations whose motion, although steady in time, departed from the regional velocity pattern.

San Juan Bautista, California: Small ($M < 3.7$) Earthquakes Embedded in an Aseismic Slip Episode, December 1992

San Juan Bautista is located along the creeping section of the San Andreas Fault (**Figure 7*a***), where the surface fault trace displaces in a combination of steady and

episodic creep at approximately 30 mm year^{-1}. During the seven-year period studied by Gladwin et al. (1994), from February 15, 1985, to June 7, 1992, the SJT three-component borehole strainmeter (**Figure 7*a***) recorded 15 episodes of accelerated aseismic strain, 14 of which were followed within hours to days by accelerated fault creep as measured by a creepmeter spanning the fault 2 km southeast of the strainmeter. The strain events typically lasted 1 h, had amplitudes of several tens of nanostrain, and with one exception can be modeled as resulting from right-lateral strike slip of a patch on the San Andreas Fault extending between depths of 200 and 500 m. None of these strain events was accompanied by earthquakes and no signals were recorded at the borehole dilatometer located 6 km to the northeast.

On December 11, 1992, a much larger and longer-duration slow strain event began (**Figure 7*c***; Linde et al. 1996). This distinctive episode lasted about a week, was recorded at both San Juan Bautista and Searle Road, and accompanied a unique sequence of small earthquakes on the San Andreas Fault between the two strainmeters. The first earthquake (M_L3.1) preceded the onset of the strain event by about 2 h; subsequent earthquakes were preceded and/or followed by rapid strain rate changes, although the 10- and 18-min sampling intervals for the dilatometer and three-component strainmeter preclude determining the precise time relation between the earthquakes and strain changes. Linde et al. (1996) modeled the strain signals assuming a sequence of right-lateral slip events on fault patches between the two strainmeters, with total moment equivalent to a M4.8 earthquake. Their preferred model places the slip above the 4–8 km depths of the earthquake hypocenters, but the data permit slip extending to greater depths. Estimated coseismic strain from the small earthquakes accounts for a negligible proportion of the aseismic strain. The episode exemplifies the occurrence of seismic rupture during a period of aseismic fault failure. In contrast to aseismic slip events downdip of subduction zone earthquake sources, this slow earthquake sequence represents slip that is shallower than earthquake hypocenters.

Creep Events and M > 3.5 Earthquakes on the San Andreas Fault

Thurber & Sessions (1998) assessed whether accelerated fault creep could provide useful warnings of earthquakes along 75 km of the creeping section of the San Andreas Fault in central California. For the period 1980 to 1996, they concluded that during time windows of 5 to 10 days following creep events, earthquakes of M3.5 and above were significantly more likely (probability gains of up to 3) than uniform background probabilities. However, they also found that 88%–94% of the creep events were false alarms, in that no M3.5 or greater earthquake occurred within the next 5–10 days. Interestingly, the earthquakes that did fall within the specified time windows following creep events were not necessarily near the creepmeter where the creep event occurred. They speculated that fault creep events might often be associated with seismic fault slip at depth, as for the December 1992 slow earthquake recorded by the San Juan Bautista borehole strainmeter.

The 1999 Chi-Chi, Taiwan, Earthquake (M_w7.6): No Preseismic Deformation Rate Change Detected

The 1999 M_w7.6 Chi-Chi earthquake nucleated at 8 km depth and produced surface offsets along 100 km of the shallowly dipping Chelungpu thrust fault, with scarps up to 8 m high (Shin & Teng 2001). Forty-one CGPS stations were operating on the island of Taiwan and on other islands within 50 km of Taiwan at the time of the mainshock. No change in pre-earthquake deformation rate was observed at any station. Coseismic displacement was 1.9 m at the nearest station, SUNM, 10 km NE of the epicenter (Yu et al. 2001). Coseismic displacements in excess of 0.1 m were observed at five additional stations within 100 km of the rupture zone. To produce 0.01 m of displacement (0.5% of the mainshock coseismic displacement) at SUNM, the moment of aseismic slip would have needed moment equivalent to a M6 earthquake, assuming its distribution was similar to that in the mainshock. Deeper slip would have needed to have a larger moment to be detected.

Corinth Rift, Greece: Accelerating Strain Before a M3.5 Earthquake in 2002

Bernard et al. (2004) report a 0.1 microstrain contractional transient lasting about 1 h prior to the arrival of seismic waves from a M3.5 earthquake 14 km away, recorded by a borehole dilatometer installed at 148 m depth on Trizonia Island in the Gulf of Corinth, Greece (**Figures 8*a*** and **8*b***). The M3.5 earthquake, on December 3, 2002, was the largest event of a seismic swarm that had begun 13 days earlier and persisted for several weeks. If the strain transient resulted from a slow slip event near the M3.5 earthquake, then moment equivalent to a M5.3 earthquake is required. Bernard et al. (2004) note that the decay of the transient signal is inconsistent with unidirectional slip on a single fault plane, and could indicate fluid flow, propagation of the source, or activation of a second fault. The observation of strain other than a coseismic step with only one event of a swarm is similar to the situation in 1997 at Long Valley Caldera, where only the largest (M4.9) of hundreds of events in a swarm lasting several months produced a large strain and fluid pressure transient (Roeloffs et al. 2003). Hill et al. (2003) show that this M4.9 event likely represented upward propagation of magmatic fluid. More information about the Gulf of Corinth earthquake swarm would help with interpretation of the strain transient, which may be related to magmatic processes.

Critical evaluation of this signal is difficult because it was below the resolution of other crustal deformation sensors on Trizonia. Although routine variations in the strain data are as large as the pre-earthquake transient, the steep rise time of the transient distinguishes it from noise. The decay of the transient is slower, however, and therefore more similar to background noise than its onset.

The 2004 Parkfield, California, Earthquake (M_w6.0): No Preseismic Deformation Rate Change Detected

In 1985, the USGS began intensified monitoring of the Parkfield segment of the San Andreas Fault in central California, prompted by the history of remarkably similar

Figure 8

(*a*) Map showing location of Trizonia Island and M3.5 earthquake in the Gulf of Corinth, Greece. (*b*) Data from dilatometer on Trizonia Island, showing successively expanded views of deformation before, during, and after the M3.5 earthquake on December 3, 2002. Strain data are recorded continuously at 5 Hz and triggered data are recorded at 50 Hz.

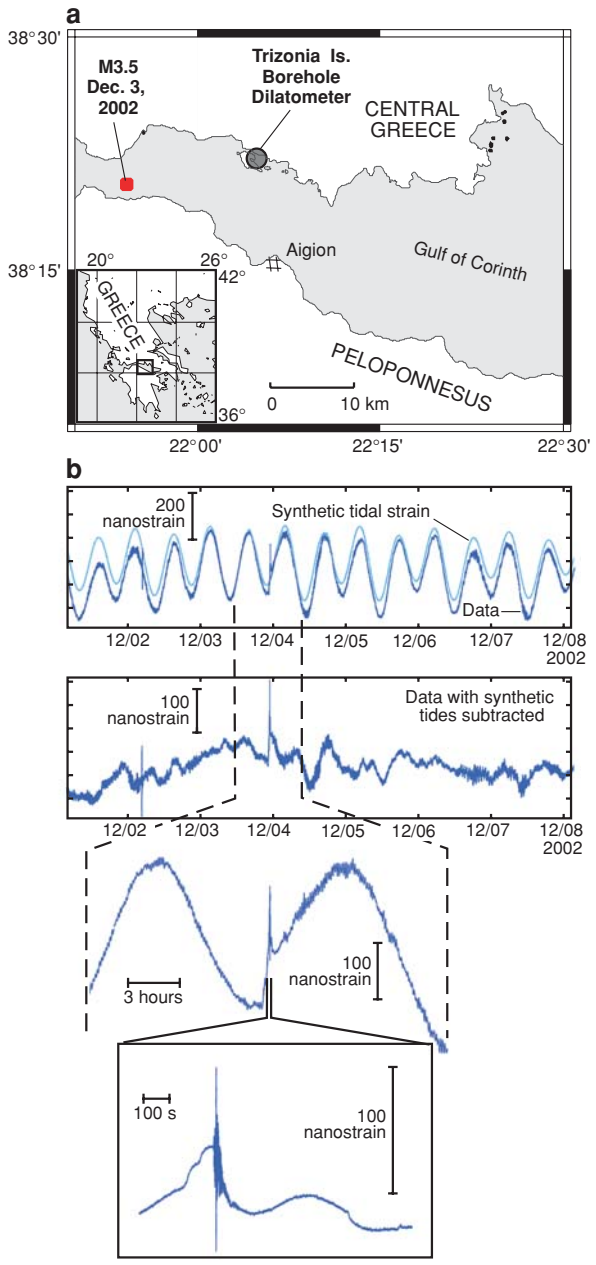

M6 earthquakes there in 1857, 1881, 1901, 1922, 1934, and 1966, and the conjecture (Bakun & Lindh 1985) that another M6 event would recur before 1993. The anticipated M6 Parkfield earthquake finally took place on September 28, 2004, with no pre-earthquake changes in deformation rate recognized beforehand or identified through analysis to date. Roeloffs & Langbein (1994) and Roeloffs (2000) review this experiment and describe the evolution of instrumentation. Langbein et al. (2005) and Bakun et al. (2005) summarize early postearthquake results.

Unique crustal deformation instrumentation at Parkfield included 12 creepmeters, a dual-frequency electronic distance meter (two-color EDM), eight dilatometers, and three three-component strainmeters in boreholes 170–320 m deep. By September 2004, three dilatometers and one three-component borehole strainmeter had ceased working, among them the two Gold Hill dilatometers that would have been closest to the 2004 Parkfield epicenter, which had recorded contractional strain prior to the 1985 Kettleman Hills earthquake. Monitoring of the water wells that had shown preseismic changes prior to the 1985 Kettleman Hills earthquake had also been discontinued. The two-color EDM measurements were being made less frequently, and CGPS stations had been installed at most monuments. Despite these changes, the 2004 Parkfield earthquake provided borehole strainmeter recordings closer to a M6 hypocenter than any previous earthquake worldwide.

No significant changes in crustal deformation rates were detected in the weeks or minutes prior to the 2004 Parkfield earthquake (**Figures 9*a*,*b*,*c***). Data from the Frolich dilatometer plotted in Langbein et al. (2005) include a step-like change of about 10 nanostrain 24 h before the earthquake, but this has been shown to be an artifact resulting from resetting of a valve (J. Langbein, personal communication, 2004). Higher-frequency recording of the dilatometer data showed no changes exceeding 0.1 nanostrain in the 20 s prior to the earthquake, constraining moment release near the hypocenter during this time period to less than the equivalent of a M3.2 earthquake. The 2004 Parkfield earthquake had no foreshocks, in contrast to the 1966 Parkfield earthquake, which did have a foreshock and anecdotal reports of pre-earthquake surface slip.

The interseismic slip rate of the San Andreas Fault near Parkfield varied between the 1966 and 2004 earthquakes. In particular, a higher slip rate between 1992 and 1995 was detected by three-component borehole strainmeters (Gwyther et al. 1996) and the two-color EDM (Langbein et al. 1999), and accompanied by a faster recurrence of repeating microearthquakes (Nadeau & McEvilly 1999). Three $M > 4$ earthquakes also occurred near the 1966 Parkfield mainshock hypocenter during this period. However, the fault slip rate subsequently returned to preanomaly values, illustrating that changes in interseismic deformation rates are not necessarily earthquake precursors.

THE IZU PENINSULA, JAPAN: DEFORMATION DRIVEN BY MAGMATIC PROCESSES

The Izu peninsula on the Pacific coast of Honshu is the most volcanically and seismically active area of Japan, and crustal deformation monitoring has been carried out there since the mid-1970s. Earthquake swarms related to volcanic activity off the east

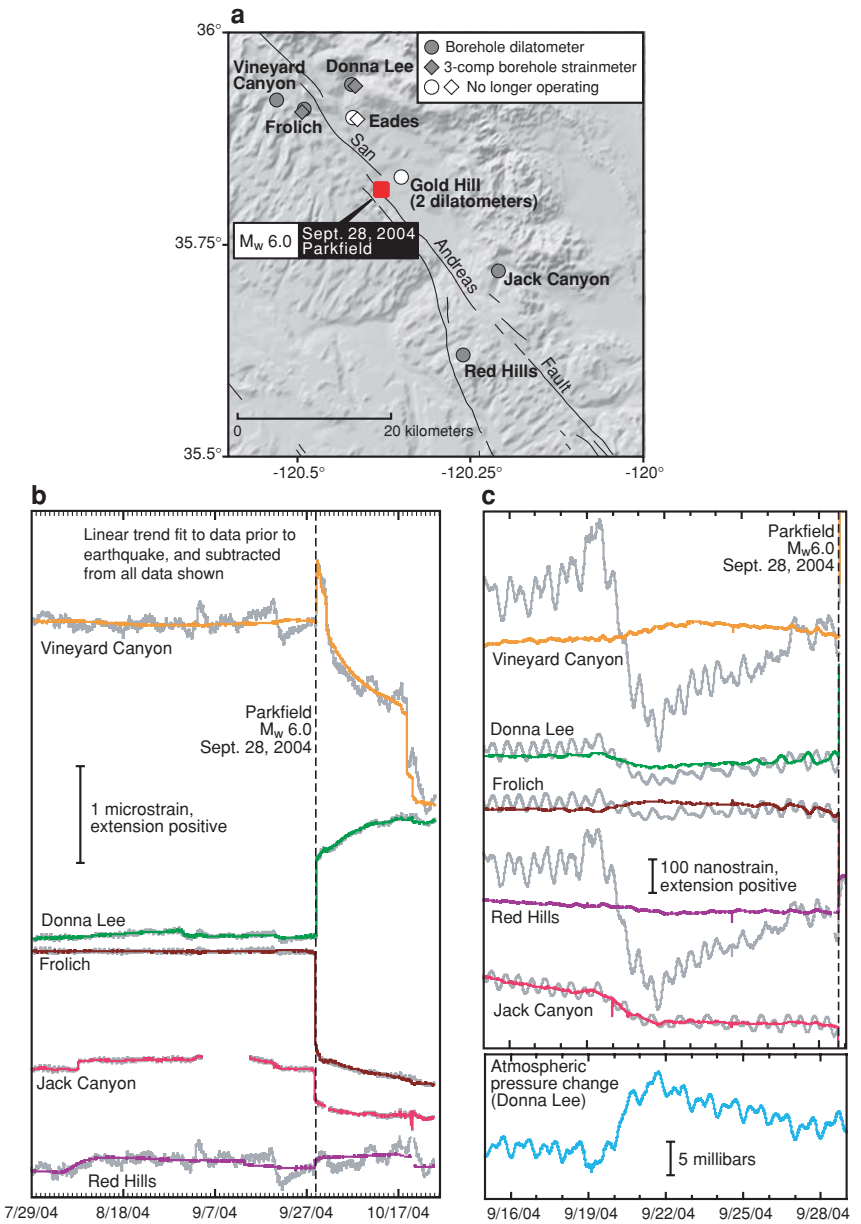

Figure 9

(*a*) Map showing locations of borehole strainmeters near Parkfield, California. (*b*) Data from Parkfield dilatometers for a three-month period prior to the 2004 Parkfield earthquake. Data collected by USGS. Gray curves are cleaned data, colored curves have been corrected for variations induced by Earth tides and atmospheric pressure. A linear time function has been fitted to the data prior to the earthquake and then subtracted from all of the data shown. (*c*) Same as (*b*) for the period September 15–29, 2004. Coseismic strains are off the scale of this plot.

coast of the Izu peninsula occurred frequently from 1975 to 1989, and in 1989 an intensive swarm was associated with the Ito-oki submarine eruption (Ukawa & Tsukahara 1996). Swarms have continued to occur, and Koizumi et al. (1999) show that at least four of these swarms have been preceded by strain rate changes, as measured with borehole strainmeters and high-resolution groundwater level observations. The reason why crustal deformation changes are detectable is that the earthquake swarms are driven by dike intrusion (Koizumi et al. 1999).

On January 14, 1978, a M7.0 (M_w6.0) earthquake, the Izu-Oshima Kinkai earthquake, took place between Izu Oshima Island and the Izu peninsula. The part of the rupture on the peninsula is described as right-lateral strike-slip by Inouchi & Sato (1979), but the Harvard CMT catalog shows a component of dip slip to the faulting (**http://www.seismology.harvard.edu/CMTsearch.html**). Leveling and tide-gauge measurements revealed that 15 cm of uplift had taken place between 1974 and 1976 near the western end of the rupture zone (Inouchi & Sato 1979). In the five years prior to the earthquake, geodetic lines between the peninsula and Izu Oshima Island lengthened 5–6 cm. Wakita (1981) noted that groundwater levels in several monitoring wells dropped, beginning two to five weeks prior to the earthquake. The observations are all consistent with an area of crustal expansion north of the rupture.

The Izu peninsula is a unique setting where seismicity is largely driven by magmatic activities such as dike intrusion, which deform Earth's crust (e.g., Aoki et al. 1999). The geodetic and continuous strain observations on the Izu peninsula are critical for characterizing the behavior of this hazardous populated area, but similar observations of pre-earthquake deformation probably cannot be expected in tectonic settings without magmatic activity.

OCEANIC TRANSFORM FAULTS

Broadband triaxial seismometers with high dynamic range facilitate the analysis of free oscillations and surface waves to characterize the rupture histories of large earthquakes at periods as long as 1000 s. Since the 1960 Chile earthquake, slow precursors lasting tens to hundreds of seconds have been found almost exclusively for strike-slip earthquakes on oceanic transform faults. Several of the examples are controversial.

The May 23, 1989, Macquarie Ridge earthquake (M_w8.2), beneath the Pacific Ocean about 1000 km south of New Zealand, was one of the first great earthquakes recorded on a large number of broadband seismic stations. Ihmlé et al. (1993) described this event as a "fast-rupturing ordinary earthquake initiated by an episode of slow, smooth deformation that began more than 100 s before the main shock," based on 1–50 mHz seismic waves. The slow precursor had estimated moment equivalent to a M7.6 earthquake, and was not discernible in P-wave arrivals from the closest stations ($\Delta = 30°$–$34°$), implying it had a smooth time function. The data weakly indicate that the slow precursor's centroid was deeper than the 23 km depth determined for the entire earthquake.

For the March 14, 1994, M_w7.0 Romanche transform earthquake, beneath the equatorial Atlantic Ocean, McGuire et al. (1996) interpreted a ramp in low-passed seismograms preceding the P-wave arrival, observed at six broadband seismic

stations, as time-domain evidence for a 100-s slow precursor with moment equivalent to M_w6.4. The Romanche transform earthquake comprised at least two subevents; McGuire et al. (1996) located the second of these on a separate fault 80 km northeast of the main transform. McGuire & Jordan (2000) obtained a similar result for the April 28, 1997, Prince Edward Island earthquake (M_w6.8), beneath the Indian Ocean on the Discovery II transform fault southeast of Africa, finding this to have initiated with a slow event beginning 15 s before the mainshock. By supplementing Global Seismograph Network (GSN) data with recordings from a temporary broadband deployment in southern Africa, they located the mainshock beneath a separate, but parallel, seafloor valley, 40 km from the slow earthquake's epicenter in the main Discovery II transform.

An important alternative viewpoint is that of Abercrombie & Ekström (2001, 2003), who argue that slow precursors and slip on spatially separated faults are artifacts of analyses that assume shallow depths and inappropriate velocity models. Assuming a deeper source, they successfully modeled body wave seismograms of the 1994 Romanche transform earthquake without a slow precursor and/or slip on a separate fault. They question data quality for the 1997 Prince Edward Island earthquake and cite studies of the 1989 Macquarie Ridge earthquake, which found no slow precursor.

Independent support for the idea that oceanic transform earthquakes involve coupled events on separate faults was obtained by Forsyth et al. (2003), who used ocean-bottom seismometer observations and data from one GSN station to study a 4.5-h, 60-event swarm of strike-slip earthquakes on the western boundary of the Easter microplate, beneath the South Pacific Ocean. The small events (maximum magnitude 4.9) alternated randomly between two transform faults 25 km apart. Because neither static nor dynamic stress changes imposed by such small events could explain coupling between the two transforms, Forsyth et al. (2003) concluded that an aseismic event "undetectable with ordinary seismological techniques" drove the swarm.

McGuire et al. (2005) used data from a submarine hydroacoustic array to study seismicity of the East Pacific Rise, where transform faults host earthquakes as large as M6.5, but accommodate an estimated 85% of plate motion aseismically. High rates of foreshocks occur within an hour prior to many mainshocks, possibly indicating extended aseismic preparation periods.

The June 2000 earthquake sequence in the South Iceland Seismic Zone, where parts of a spreading center and associated transform faults continue onshore, had features attributed to oceanic transform seismicity. Within 5 min of a M_w6.5 earthquake on June 17, 2000, several M5 triggered earthquakes occurred on separate faults 60–80 km to the west (Árnadóttir et al. 2004). One of the triggered events appeared to involve significant aseismic slip, based on its relatively large geodetic moment. On June 21, a M_w6.4 earthquake took place 20 km west of the June 17 epicenter. Possible pre-earthquake deformation was suggested in preliminary reports (Stefánsson et al. 2000), but judged insignificant after further analysis (T. Árnadóttir, personal communication, 2005).

DISCUSSION

There are at least ten credible examples of earthquakes in nonmagmatic settings preceded by deformation rate changes (**Table 1**). Eight of the examples predate the deployment of modern CGPS networks. Seven of these earthquakes were of magnitude greater than 7.5.

The paucity of positive examples based on high-quality CGPS or continuous strain data raises concerns about the validity of some of these observations. The older observations have been scrutinized, and new evidence bearing on their credibility is unlikely to emerge, but recent discoveries of large-scale aseismic slip transients in subduction zones make historical observations more plausible. Modern examples are based on data that are available to the public for further analysis.

Constraints Imposed by Observations to Date

Although some CGPS data records are now over 10 years long, and 74 earthquakes of M7.5 or greater have taken place worldwide since the beginning of 1994 (not counting aftershocks of the December 26, 2004, M_w9.2 Sumatra-Andaman earthquake), only about 12 of these large events occurred within 200 km of even one CGPS station. At that distance, even coseismic displacements can be immeasurable. However, CGPS noise levels are too high to place tight constraints on preseismic deformation rate changes even when stations are closer (**Table 2**). The tightest constraint on pre-earthquake deformation obtained to date with CGPS is $M < 6.0$ for the 1999 Chi-Chi, Taiwan, earthquake. Study of the 1999 Hector Mine earthquake shows that InSAR may be able to detect smaller pre-earthquake deformation than CGPS. The 2004 Parkfield earthquake, at M_w6.0, is significantly smaller than most earthquakes preceded by credible deformation rate changes, but because it nucleated within 10 km of a borehole dilatometer, preseismic slip with moment equivalent to a M3.2 earthquake at the hypocentral location should have been detectable. Whether this constraint is relevant to much larger earthquakes is as yet unknown.

Borehole strain data that could provide information about pre-earthquake deformation in the United States and Japan may remain to be analyzed. The deployment of more than 100 borehole strainmeters in the western United States as part of the Plate Boundary Observatory (PBO) will increase the chances of capturing data within a few kilometers of large earthquakes.

The history of CGPS or InSAR images is too short to have detected long-term changes on timescales of a decade or more, such as those inferred from microfossil data to have preceded the 1964 Alaska or 1700 Cascadia earthquakes, and strain rate changes on these timescales cannot be measured reliably in borehole strainmeter data.

Interseismic Deformation Rates are Unsteady

CGPS data acquired since the early 1990s require revising the idea that only earthquakes and postseismic slip punctuate steady interseismic strain or displacement rates. Aseismic transients in subduction zones, and the 1992–1995 Parkfield slip rate

increase, were below the resolution of geodolite or campaign GPS measurements. Such variations were thus undetectable prior to the early 1990s.

The new challenges are to distinguish among deformation rate changes owing to nontectonic influences, those that are tectonically significant, and those that might herald seismic events. Interseismic deformation rate changes require explanation. For example, to what extent can stresses imposed by large earthquakes account for strain and displacement rate changes?

Aseismic deformation now resembles seismicity: rates fluctuate and increase temporarily after large earthquakes. The data reviewed here indicate that deformation rate changes, like foreshocks, precede a subset of earthquakes.

Locations of Preseismic Deformation and Relation with Foreshocks

The majority of deformation rate changes discussed here have signs opposite to coseismic changes, or moment exceeding seismic moment, features that are inconsistent with accelerating slip on the earthquake rupture plane. It has long been proposed that pre-earthquake slip occurs in the more ductile downdip extensions of subduction interfaces, and episodic aseismic slip in Japan and Cascadia is known to occur in that setting. Aseismic deformation sources beneath the seismic rupture zone are plausible because the higher pressures and temperatures there are conducive to ductile rather than brittle deformation.

Some authors (e.g., Dodge et al. 1996, Forsyth et al. 2003) speculate that aseismic processes drive foreshock sequences. However, geodetic data have not captured such processes, and pre-earthquake crustal deformation transients have not been observed preferentially for terrestrial events with foreshocks. Of the examples reviewed here, pre-earthquake deformation rate changes and foreshocks occurred on similar timescales only for the 1960 Chile, 1983 Japan Sea, 1985 Kettleman Hills, and possibly the 1964 Alaska earthquakes. Foreshocks might not be expected to accompany aseismic pre-earthquake deformation that originates below brittle seismogenic depths (Ohnaka 1992).

Timescales

Pre-earthquake deformation rate changes take place over timescales ranging from hundreds of seconds to over a decade (**Table 1**). In the context of faults whose frictional strength can be modeled as rate and state dependent, this range of timescales may reflect differences in the distribution of the characteristic slip distance, L. Laboratory values of L (typically 10^{-5} m) can account for preinstability slip lasting seconds or less, whereas simulations such as that of Kuroki et al. (2004) for Tokai show that if $L = 5$–15 cm, transient aseismic slip lasting over 10 years is expected. Lapusta & Rice (2003) argue, however, that laboratory-measured values of L account well for the sizes of the smallest earthquakes. Controversy regarding the ubiquity of slow slip preceding oceanic transform earthquakes needs to be resolved because, if real, these observations suggest the frictional properties of faults in this setting may be unique.

Future Directions

The examples here imply large ($M > 8$) earthquakes in subduction zones are the best targets for instrumentation. The instrumentation should include borehole strainmeters in addition to CGPS, and must be as close as possible to anticipated earthquake source zones, ideally within a few kilometers. Seafloor GPS (Spiess et al. 1998, Osada et al. 2003) and submarine boreholes instrumented with fluid pressure sensors (Davis et al. 2001) and borehole strainmeters (Araki et al. 2004) will advance characterization of aseismic deformation around subduction zones.

Terrestrial earthquakes in nonmagmatic settings have yielded relatively few examples of pre-earthquake deformation rate changes (**Tables 1** and **2**). These smaller magnitude earthquakes may have smaller pre-earthquake signals. Perhaps more importantly, aseismic transient deformation has not yet been observed in most of these settings, or, in the case of the San Andreas Fault, such transient deformation occurs primarily at shallow depths.

The current state of knowledge does not require earthquake scientists to conclude that all earthquakes are unpredictable. While the unpredictable earthquake is an essential scenario for public safety planning, the growing stream of real-time crustal deformation data challenges earthquake scientists to identify and interpret deformation rate changes that might indicate heightened hazard. Diverse data sets and analyses by individual researchers need to be evaluated collaboratively on a regular basis, as is done by the CCEP in Japan. The ambitious Tokai earthquake prediction effort could be a watershed for research and policy in this area, regardless of its outcome.

ACKNOWLEDGMENTS

Review comments by Tom Brocher and Mary Lou Zoback led to substantial improvements in this paper. I also thank T. Árnadóttir, P. Bernard, J. Langbein, and T. Melbourne for helpful information and discussion.

LITERATURE CITED

Abercrombie R, Mori J. 1994. Local observations of the onset of a large earthquake: 28 June 1992 Landers, California. *Bull. Seismol. Soc. Am.* 84:725–34

Abercrombie R, Ekström G. 2001. Earthquake slip on oceanic transform faults. *Nature* 410:74–77

Abercrombie R, Ekström G. 2003. A reassessment of the rupture characteristics of oceanic transform faults. *J. Geophys. Res.* 108:doi:10.1029/2001JB000814

Agnew DC. 1986. Strainmeters and tiltmeters. *Rev. Geophys.* 24:579–624

Aoki Y, Segall P, Kato T, Cervelli P, Shimada S. 1999. Imaging magma transport during the 1997 seismic swarm off the Izu peninsula, Japan. *Science* 286:927–30

Araki E, Shinohara M, Sacks S, Linde A, Kanazawa T. 2004. Improvement of seismic observation in the ocean by use of seafloor boreholes. *Bull. Seismol. Soc. Am.* 94:678–90

Árnadóttir T, Geirsson H, Einarsson P. 2004. Coseismic stress changes and crustal deformation on the Reykjanes peninsula due to triggered earthquakes on 17 June 2000. *J. Geophys. Res.* 109:B09307, doi:10.1029/2004JB003130

Atwater BF. 1996. Coastal evidence for great earthquakes in western Washington. In *Assessing Earthquake Hazards and Reducing Risk in the Pacific Northwest*, *USGS Prof. Pap. 1560* 1:77–90, Reston, VA

Austin KE, Miller MM. 2002. The coseismic displacement fields for the 1992 Landers and 1999 Hector Mine earthquakes in California, from regional GPS observations. *Bull. Seismol. Soc. Am.* 92:1365–76

Bakun WH, Aagard B, Dost B, Ellsworth WL, Hardebeck JL, et al. 2005. Implications for prediction and hazard assessment from the 2004 Parkfield earthquake. *Nature* 437:969–74

Bakun WH, Lindh AG. 1985. The Parkfield, California, earthquake prediction experiment. *Science* 229:619–24

Bernard P, Boudin F, Sacks S, Linde A, Blum P-A, et al. 2004. Continuous strain and tilt monitoring on the Trizonia Island, Rift of Corinth, Greece. *C.R. Geosci.* 335:313–23

Beroza GA, Ellsworth WL. 1996. Properties of the seismic nucleation phase. *Tectonophysics* 261:209–27

Cifuentes IL. 1989. The 1960 Chilean earthquake. *J. Geophys. Res.* 94:665–80

Cifuentes IL, Silver PG. 1989. Low-frequency source characteristics of the great 1960 Chilean earthquake. *J. Geophys. Res.* 94:643–63

CCEP. 2005. **http://cais.gsi.go.jp/YOCHIREN/JIS/162/image162/004_5.pdf**

Davis EE, Wang K, Thomson RE, Becker K, Cassidy JF. 2001. An episode of seafloor spreading and associated plate deformation inferred from crustal fluid pressure transients. *J. Geophys. Res.* 106:21953–64

Dieterich JA. 1992. Earthquake nucleation on faults with rate- and state-dependent strength. *Tectonophysics* 211:115–34

Dodge DA, Beroza GC, Ellsworth WL. 1996. Detailed observations of California foreshock sequences: implications for the earthquake initiation process. *J. Geophys. Res.* 101:22371–92

Doser DI, Brown WA. 2001. A study of historic earthquakes of the Prince William Sound, Alaska, region. *Bull. Seismol. Soc. Am.* 91:842–57

Dragert H, Wang K, James TS. 2001. A silent slip event on the deeper Cascadia subduction interface. *Science* 292:1525–28

EERI Committee on the Anticipated Tokai Earthquake, Scawthorn C, ed. 1984. *Anticipated Tokai Earthquake: Japanese Prediction and Preparedness Activities*. Oakland, CA: EERI. 89 pp.

Ekström G, Stein RS, Eaton JP, Eberhart-Phillips D. 1992. Seismicity and geometry of a 110-km-long blind thrust fault 1. The 1985 Kettleman Hills, California, earthquake. *J. Geophys. Res.* 97:4843–64

Forsyth DW, Yang Y, Mangriotis MD. 2003. Coupled seismic slip on adjacent oceanic transform faults. *Geophys. Res. Lett.* 30:1618, doi:10.1029/2002GL016454

Gladwin MT, Gwyther RL, Hart RHG, Breckenridge KS. 1994. Measurements of the strain field associated with episodic creep events on the San Andreas Fault at San Juan Bautista, California. *J. Geophys. Res.* 99:4559–65

Gladwin MT, Gwyther RL, Higbie JW, Hart RHG. 1991. A medium term precursor to the Loma Prieta earthquake? *Geophys. Res. Lett.* 18:1377–80
Gwyther RL, Gladwin MT, Mee M, Hart RHG. 1996. Anomalous tensor strain at Parkfield during 1993–1994. *Geophys. Res. Lett.* 23:2425–28
Hamilton S, Shennan I. 2005a. Late Holocene great earthquakes and relative sea level change at Kenai, southern Alaska. *J. Quat. Sci.* 20:95–111
Hamilton S, Shennan I. 2005b. Late Holocene relative sea level changes and the earthquake deformation cycle around upper Cook Inlet, Alaska. *Quat. Sci. Rev.* 24:1479–98
Hauksson E, Jones LM, Hutton K, Eberhart-Phillips D. 1993. The 1992 Landers earthquake sequence: seismological observations. *J. Geophys. Res.* 98:19835–58
Hauksson E, Jones LM, Hutton K. 2002. The 1999 M_w7.1 Hector Mine, California, earthquake sequence: complex conjugate strike-slip faulting. *Bull. Seismol. Soc. Am.* 92:1154–70
Hemphill-Haley E. 1995. Diatom evidence for earthquake-induced subsidence and tsunami 300 yr ago in southern coastal Washington. *Geol. Soc. Am. Bull.* 107:367–78
Hill DP, Langbein JO, Prejean S. 2003. Relations between seismicity and deformation during unrest in Long Valley Caldera, California, from 1995 through 1999. *J. Volc. Geotherm. Res.* 127:175–93
Ihmlé PF, Harabaglia P, Jordan TH. 1993. Teleseismic detection of a slow precursor to the great 1989 Macquarie Ridge earthquake. *Science* 261:177–83
Ihmlé PF, Jordan TH. 1994. Teleseismic search for slow precursors to large earthquakes. *Science* 266:1547–51
Iio Y, Kobayashi Y, Tada T. 2002. Large earthquakes initiate by the acceleration of slips on the downward extensions of seismogenic faults. *Earth Planet. Sci. Lett.* 202:337–43
Inouchi N, Sato H. 1979. Crustal deformation related to the Izu-Oshima Kinkai earthquake of 1978. *Bull. Geographical Surv. Inst.* 23:14–24
Irwan M, Kimata F, Hirahara K, Sagiya T, Yamagiwa A. 2004. Measuring ground deformations with 1-Hz GPS data: the 2003 Tokachi-oki earthquake (preliminary report). *Earth Planet. Space* 56:389–93
Johnston MJS, ed. 1993. The Loma Prieta, California, earthquake of October 17, 1989—Preseismic observations. In *U.S. Geological Survey Prof. Pap. 1550-C.* Washington, DC: United States Gov. Print. Off.
Johnston MJS, Linde AT. 1993. Near-field high-resolution strain measurements. See Johnston 1993, pp. C53–58
Johnston MJS, Linde AT, Agnew DC. 1994. Continuous borehole strain in the San Andreas Fault zone before, during, and after the 28 June 1992 M_w7.3 Landers, California, earthquake. *Bull. Seismol. Soc. Am.* 84:799–805
Johnston MJS, Linde AT, Gladwin MT. 1990. Near-field high resolution strain measurements prior to the October 18, 1989, Loma Prieta Ms 7.1 earthquake. *Geophys. Res. Lett.* 17:1777–80
Johnston MJS, Linde AT, Gladwin MT, Borcherdt RD. 1987. Fault failure with moderate earthquakes. *Tectonophysics* 144:189–206

Kanamori H, Anderson DL. 1975. Amplitude of the Earth's free oscillations and long-period characteristics of the earthquake source. *J. Geophys. Res.* 80:1075–78

Kanamori H, Cipar JJ. 1974. Focal process of the great Chilean earthquake, May 22, 1960. *Phys. Earth Planet. Int.* 9:128–36

Kobayashi A, Manago N, Yoshida A. 2002. Sea level changes just before the 1946 Nankai earthquake. *J. Geodetic. Soc. Jpn.* 48:1–12

Koizumi N, Tsukuda E, Kamigaichi O, Matsumoto N, Takahashi M, Sato T. 1999. Preseismic changes in groundwater level and volumetric strain associated with earthquake swarms off the east coast of the Izu Peninsula, Japan. *Geophys. Res. Lett.* 26:3509–12

Kuroki K, Ito HM, Takayama H, Yoshida A. 2004. 3-D simulation of the occurrence of slow slip events in the Tokai region with a rate- and state-dependent friction law. *Bull. Seismol. Soc. Am.* 94:2037–50

Langbein JO, Borcherdt R, Dreger D, Fletcher J, Hardebeck J. 2005. Preliminary report on the 28 September 2004, M 6.0 Parkfield, California, earthquake. *Seis. Res. Lett.* 76:10–26

Langbein JO, Gwyther RL, Hart RHG, Gladwin MT. 1999. Slip rate increase at Parkfield in 1993 detected by high-precision EDM and borehole tensor strainmeters. *Geophys. Res. Lett.* 26:2529–32

Langbein JO, Johnson H. 1997. Correlated errors in geodetic time series: implications for time-dependent deformation. *J. Geophys. Res.* 102:591–603

Langbein JO, Quilty E, Breckenridge K. 1993. Sensitivity of crustal deformation instruments to changes in secular rate. *Geophys. Res. Lett.* 20:85–88

Lapusta N, Rice JR. 2003. Nucleation and early seismic propagation of small and large events in a crustal earthquake model. *J. Geophys. Res.* 108:2205, doi: 10.1029/2001JB000793

Larsen CF, Echelmeyer KA, Freymueller JT, Motyka RJ. 2003. Tide records of uplift along the Northern Pacific-North American plate boundary, 1937–2001. *J. Geophys. Res.* 108:doi:10.1029/2001JB001685

Linde AT, Gladwin MT, Johnston MJS. 1993. Borehole strain measurements of solid-earth-tidal amplitudes. See Johnston 1993, pp. C81–85

Linde AT, Gladwin MT, Johnston MJS, Gwyther RL, Bilham RG. 1996. A slow earthquake sequence on the San Andreas Fault. *Nature* 383:65–68

Linde AT, Sacks IS. 2002. Slow earthquakes and great earthquakes along the Nankai Trough. *Earth Planet. Sci. Lett.* 203:265–75

Linde AT, Silver PG. 1989. Elevation changes and the great 1960 Chilean earthquake: support for aseismic slip. *Geophys. Res. Lett*. 16:1305–8

Linde AT, Suyehiro K, Miura S, Sacks IS, Takagi A. 1988. Episodic aseismic earthquake precursors. *Nature* 334:513–15

Lisowski M, Prescott W, Savage J, Svarc JL. 1990. A possible geodetic anomaly observed prior to the Loma Prieta, California, earthquake. *Geophys. Res. Lett.* 17:1211–14

Lisowski M, Savage JC, Prescott WH, Svarc JL, Murray MH. 1993. No convincing precursory geodetic anomaly observed. See Johnston 1993, pp C67–72

Lyons S, Sandwell D. 2003. Fault creep along the southern San Andreas from interferometric synthetic aperture radar, permanent scatterers, and stacking. *J. Geophys. Res.* 108:doi:10.1029/2002JB001831
Mazzotti S, Adams J. 2004. Variability of near-term probability for the next great earthquake on the Cascadia subduction zone. *Bull. Seismol. Soc. Am.* 94:1954–59
McGuire JJ, Boettcher MS, Jordan TH. 2005. Foreshock sequences and short-term earthquake predictability on East Pacific Rise transform faults. *Nature* 434:457–61
McGuire JJ, Ihmlé PF, Jordan TH. 1996. Time-domain observations of a slow precursor to the 1994 Romanche transform earthquake. *Science* 274:82–85
McGuire JJ, Jordan TH. 2000. Further evidence for the compound nature of slow earthquakes: the Prince Edward Island earthquake of April 28, 1997. *J. Geophys. Res.* 105:7819–27
Melbourne TE, Webb FH. 2002. Precursory transient slip during the 2001 $M_w = 8.4$ Peru earthquake sequence from continuous GPS. *Geophys. Res. Lett.* 29:doi:10.1029/2002GL015533
Mellors RJ, Sichoix L, Sandwell DT. 2002. Lack of precursory slip to the 1999 Hector Mine, California, earthquake as constrained by InSAR. *Bull. Seismol. Soc. Am.* 92:1443–49
Miller MM, Melbourne TJ, Johnson DJ, Summer WQ. 2002. Periodic slow earthquakes from the Cascadia subduction zone. *Science* 295:2423
Miura S, Suwa Y, Hasegawa A, Nishimura T. 2004. The 2003 M8.0 Tokachi-Oki earthquake—how much has the great event paid back slip debts? *Geophys. Res. Lett.* 31:L05613, doi:10.1029/2003GL019021
Mogi K. 1985. Precursors of the 1983 Japan Sea earthquake. *Earthq. Predict. Res.* 3:493–517
Murai Y. 2003. Delamination structure imaged in the source area of the 1982 Urakawa-oki earthquake. *Geophys. Res. Lett.* 30:1490, doi:10.1029/2002GL016459
Nadeau RM, McEvilly TV. 1999. Fault slip rates at depth from recurrence intervals of repeating microearthquakes. *Science* 285:718–21
Nelson AR, Jennings AE, Kashima K. 1996. An earthquake history derived from stratigraphic and microfossil evidence of relative sea-level change at Coos Bay, southern coastal Oregon. *Geol. Soc. Am. Bull.* 108:141–54
Ohnaka M. 1992. Earthquake source nucleation; a physical model for short-term precursors. *Tectonophysics* 211:149–78
Okada Y. 1985. Surface deformation due to shear and tensile faults in a half space. *Bull. Seismol. Soc. Am.* 75:1135–54
Okal EA, Newman AV. 2001. Tsunami earthquakes; the quest for a regional signal. *Phys. Earth Planet. Int.* 124:45–70
Osada Y, Fujimoto H, Miura S, Sweeney A, Kanazawa T. 2003. Estimation and correction for the effect of sound velocity variation on GPS/acoustic seafloor positioning; an experiment off Hawaii Island. *Earth Planet. Space* 55:e17–20
Ozawa S, Murakami M, Kaidzu M, Tada T, Sagiya T, et al. 2002. Detection and monitoring of ongoing aseismic slip in the Tokai region, central Japan. *Science* 298:1009–12

Ozawa S, Murakami M, Tada T. 2001. Time-dependent inversion study of the slow thrust event in the Nankai trough subduction zone, southwestern Japan. *J. Geophys. Res.* 106:787–802

Perez OJ, Scholz CH. 1997. Long-term seismic behavior of the focal and adjacent regions of great earthquakes during the time between two successive shocks. *J. Geophys. Res.* 102:8203–16

Quilty E, Roeloffs E. 1997. Water level changes in response to the December 20, 1994 M4.7 earthquake near Parkfield, California. *Bull. Seismol. Soc. Am.* 87:310–17

Reasenberg PA. 1999. Foreshock occurrence before large earthquakes. *J. Geophys. Res.* 104:4755–68

Roeloffs E, Langbein J. 1994. The earthquake prediction experiment at Parkfield, California. *Rev. Geophys.* 32:315–36

Roeloffs E. 2000. The Parkfield, California earthquake experiment: an update in 2000. *Curr. Sci.* 79:1226–34

Roeloffs E, Sneed M, Galloway DL, Sorey ML, Farrar CD, et al. 2003. Water level changes induced by local and distant earthquakes at Long Valley caldera, California. *J. Volc. Geotherm. Res.* 127:269–303

Roeloffs E, Quilty E. 1997. Water level and strain changes preceding and following the August 4, 1985 Kettleman Hills, California, earthquake. *Pure Appl. Geophys.* 149:21–60

Rogers G, Dragert H. 2003. Episodic tremor and slip on the Cascadia subduction zone: the chatter of silent slip. *Science* 300:1942–43

Sagiya T. 1998. Crustal movements as earthquake precursors—leveling anomaly before the 1944 Tonankai earthquake revisited. *Bull. Geogr. Surv. Inst.* 44:23–36

Satake K, Shimazaki K, Tsuji Y, Ueda K. 1996. Time and size of a giant earthquake in Cascadia inferred from Japanese tsunami records of January 1700. *Nature* 379:246–49

Sato H. 1982. On the changes in the sea level at Tosashimizu before the Nankaido earthquake of 1946. *J. Seismol. Soc. Japan* 35:623–26

Savage JC, Plafker G. 1991. Tide gauge measurements of uplift along the south coast of Alaska. *J. Geophys. Res.* 96:4325–35

Segall P, Davis JL. 1997. GPS applications for geodynamics and earthquake studies. *Annu. Rev. Earth Planet. Sci.* 25:301–36

Shearer P. 1999. *Introduction to Seismology*. Cambridge, UK: Cambridge Univ. Press

Shennan I, Long AJ, Rutherford MM, Green FM, Innes JB, et al. 1996. Tidal marsh stratigraphy, sea-level change and large earthquakes—I: a 5000 year record in Washington, USA. *Quat. Sci. Rev.* 15:1023–59

Shennan I, Long AJ, Rutherford MM, Innes JB, Green FM, Walker KJ. 1998. Tidal marsh stratigraphy, sea-level change and large earthquakes—II: submergence events during the last 3500 years at Netarts Bay, Oregon, USA. *Quat. Sci. Rev.* 17:365–94

Shennan I, Scott DB, Rutherford M, Zong Y. 1999. Microfossil analysis of sediments representing the 1964 earthquake, exposed at Girdwood Flats, Alaska, USA. *Quat. Int.* 60:55–74

Shin T-C, Teng T-L. 2001. An overview of the 1999 Chi-Chi, Taiwan, earthquake. *Bull. Seismol. Soc. Am.* 91:895–913

Spiess FN, Chadwell CD, Hildebrand JA, Young LE, Purcell GH. 1998. Precise GPS/acoustic positioning of seafloor reference points for tectonic studies. *Phys. Earth Planet. Int.* 108:101–12

Stefánsson R, Árnadóttir T, Bjornsson G, Gudmundsson GB, Halldorsson P. 2000. The two large earthquakes in the south Iceland seismic zone in June 2000: a basis for earthquake prediction research. *Eos Trans. AGU* 81:S11B-03 (Abstr.), Fall Meet. Suppl.

Takano K, Kimata F, Fujii N. 2003. Vertical ground deformation detected by the leveling and the tidal observation in Tokai region, central Japan in 1980–2002. *Eos Trans. AGU* 84:G21B-0266 (Abstr.), Fall Meet. Suppl.

Taylor DWA, Snoke JA, Sacks IS, Takanami T. 1991. Seismic quiescence before the Urakawa-oki earthquake. *Bull. Seismol. Soc. Am.* 81:1255–71

Thurber C, Sessions R. 1998. Assessment of creep events as potential earthquake precursors: application to the creeping section of the San Andreas fault, California. *Pure Appl. Geophys.* 152:685–705

Tolstoy M, Bohnenstiehl DR. 2005. Hydroacoustic constraints on the rupture duration, length, and speed of the great Sumatra-Andaman earthquake. *Seismol. Res. Lett.* 76:419–25

Ukawa M, Tsukahara H. 1996. Earthquake swarms and dike intrusions off the east coast of Izu Peninsula, central Japan. *Tectonophysics* 253:285–303

Wakita H. 1981. Precursory changes in groundwater prior to the 1978 Izu-Oshima-Kinkai earthquake. In *Earthquake Prediction: An International Review*, eds. Simpson DW, Richards PG. Am. Geophys. Union Maurice Ewing Series 4:527–32. Washington, DC: Am. Geophys. Union

Wald DJ, Helmberger DV, Heaton TH. 1991. Rupture model of the 1989 Loma Prieta earthquake from the inversion of strong-motion and teleseismic data. *Bull. Seismol. Soc. Am.* 81:1540–72

Williams SDP, Fang P, Jamason P, Nikolaidis RM, Prawirodirdjo L, et al. 2004. Error analysis of continuous GPS position time series. *J. Geophys. Res.* 109:B03412, doi:10.1029/2003JB002741

Wyatt FK, Agnew DC, Gladwin M. 1994. Continuous measurements of crustal deformation for the 1992 Landers earthquake sequence. *Bull. Seismol. Soc. Am.* 84:768–79

Wyss M, Booth DC. 1997. The IASPEI procedure for the evaluation of earthquake precursors. *Geophys. J. Intl.* 131:423–24

Yamashita T, Ohnaka M. 1992. Precursory surface deformation expected from a strike-slip fault model into which rheological properties of the lithosphere are incorporated. *Tectonophysics* 211:179–99

Yu S-B, Kuo L-C, Hsu Y-J, Su H-H, Liu C-C. 2001. Preseismic deformation and coseismic displacements associated with the 1999 Chi-Chi, Taiwan, earthquake. *Bull. Seismol. Soc. Am.* 91:995–1012

Zong Y, Shennan I, Combellick RA, Hamilton SL, Rutherford MM. 2003. Microfossil evidence for land movements associated with the AD 1964 Alaska earthquake. *Holocene* 13:7–20

Annual Review of Earth and Planetary Sciences

Volume 34, 2006

Contents